Indonesian Journal of Chemical Analysis
Homepage: https://journal.uii.ac.id/IJCA

Advances in Mesoporous Silica Nanoparticles: Synthesis, Characterization, and Biomedical Uses

Ozi Adi Saputra [a,b,c‡], Wahyu Nur Safitriono [d‡], Annisa Istiqomah [a,b], Meiyanti Ratna Kumalasari [e], Muhammad Irmawan [e], Fajar Rakhman Wibowo [d*]

[a] Department of Chemical Engineering, Collage of Engineering, National Taiwan University, Taipei, Taiwan
[b] Sustainable Chemical Science and Engineering, Taiwan International Graduate Program, Academia Sinica, Taipei, Taiwan
[c] Institute of Chemistry, Academia Sinica, Taipei, Taiwan
[d] Department of Chemistry, Faculty Mathematics and Natural Sciences, Universitas Sebelas Maret, Surakarta, Indonesia
[e] Department of Chemistry, Faculty of Mathematics and Natural Sciences, Universitas Palangka Raya, Palangka Raya, Indonesia
* corresponding author: fajarrakhman@staff.uns.ac.id

DOI: 10.20885/ijca.vol7.iss2.art9

‡ These authors contribute equally and share first authorship.

GRAPHICAL ABSTRACT

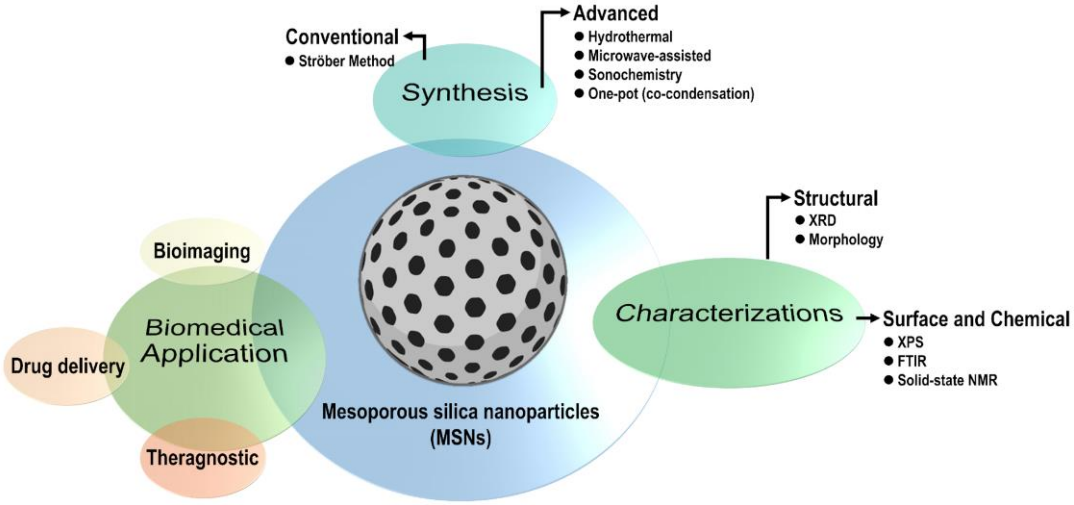

ARTICLE INFO

Received : 29 July 2024
Revised : 30 August 2024
Published : 30 September 2024
Keywords : Characterization, Drug delivery system, Nanomedicine, Mesoporous silica nanoparticle.

ABSTRACT

Mesoporous silica nanoparticles (MSNs) have drawn significant attention due to their exceptional properties and diverse range of applications, particularly in nanomedicine. The distinctive properties of MSNs, such as their high surface area, tunable pore size, and versatile surface chemistry, make them ideal candidates for various biomedical applications. This review aims to present a detailed understanding of MSNs, from synthesis and characterization to their versatile applications in biomedicine, highlighting their significant potential in advancing healthcare technologies. The synthesis methods for MSNs were comprehensively discussed, emphasizing the influence of parameters like solvent, base, alkoxysilane concentrations, and template surfactants on the size and shape of the nanostructures. Different types of MSNs, including MCM-41, SBA-15, KIT-6, and hollow MSNs, are discussed, along with their synthesis protocols and unique characteristics. The review also covers various spectroscopic techniques, such as XRD, XPS, FTIR,

NMR, and fluorescence spectroscopy, which are crucial for characterizing MSNs. Furthermore, the biomedical applications of MSNs are highlighted, demonstrating their potential in drug delivery systems, imaging, and diagnostics. The review concludes with a discussion of the future perspectives and challenges in the field, providing insights into potential developments and the prospects for clinical translation.

1. INTRODUCTION

Mesoporous silica nanoparticles (MSNs) are a type of nanomaterial that has garnered considerable interest across multiple scientific disciplines, owing to their exceptional structural features and diverse applications [1]. These nanoparticles possess a high surface area, considerable pore volume, and tunable pore sizes, which render them an outstanding platform for applications in catalysis, adsorption, and, most notably, biomedicine [2, 3]. The potential biomedical applications of MSNs are vast and varied, encompassing drug delivery, gene therapy, biosensing, and tissue engineering. Despite their impressive physical properties, the pristine MSN has limitations that prevent its direct use as a drug carrier, due to weak interactions with drug molecules resulting in premature release and reduced efficacy. Consequently, we have recently achieved significant progress in our research by manipulating the surface chemical properties of MSNs either by conjugating small molecules or polymers to control the natural release of therapeutic drugs [4-6]. The unique characteristics of MSNs, such as their ability to encapsulate and release therapeutic agents in a controlled manner, make them particularly well-suited for drug delivery systems, imaging, and tissue engineering [7]. The ability of MSNs to deliver drugs in a controlled and targeted manner has demonstrated significant potential for enhancing the efficacy and safety of therapeutic interventions. Moreover, their application in imaging and diagnostics opens up new avenues for early disease detection and treatment.

A new member of molecular sieves named M41S, classified as MSNs, was discovered in the early 1990s, encouraging research in the design of silica nanostructures for various purposes [8]. The synthesis of MSNs can be precisely controlled to tailor their size, shape, and surface properties, which are crucial factors influencing their functionality and performance in specific applications. The concentrations of water, alcoholic solvent, ammonia, alkoxysilane, and template surfactants play a pivotal role in determining the morphological and structural characteristics of the resulting silica nanostructures. Based on their structural dimensions, MSNs are divided into six forms [9]: 2D hexagonal (e.g., MCM-41) [8, 10], cubic (e.g., SBA-16) [11], 3D hexagonal (e.g., SBA-2) [12], 2D rectangular (e.g., SBA-8) [13], disordered hexagonal (e.g., MSU-1) [14], and lamellar (e.g., MSU-V) [15], with pore sizes ranging from 2 to 10 nm. MSNs are generally synthesized via surfactant template micelles, using either anionic or cationic surfactants as structure-directing agents in silica polymerization assembly [16-18]. Each template yields different silica nanostructures, resulting in varying properties such as pore size, surface area, particle size, and shape [19-21]. Nevertheless, post-synthesis modifications have been carried out for further application to enhance the versatility of MSNs by incorporating functional groups, targeting ligands, and active agents onto their surfaces [22, 23]. Wibowo et al. [24] modified the surface of MSN by poly(styrene sulfonate) which induces the pH-triggered drug release of curcumin. This strategy capable to control the release of curcumin specific to acidic environment which is a condition of cancer cells. Therefore, post-modifications are essential for optimizing the interaction of MSNs with drugs as well as biological system and improving their biocompatibility and enabling targeted drug delivery.

To fully exploit the potential of MSNs as drug carriers, it is crucial to gain detailed information about the synthesized silica nanoparticles. Spectroscopy analysis plays a vital role in this regard. X-ray diffraction (XRD) spectroscopy is suitable for obtaining initial information on the class of silica nanostructures. This review reports XRD patterns of several important classes of silica nanostructures, providing valuable references to identify synthesized silica nanoparticles. Additionally, other analytical techniques such as X-ray photoelectron spectroscopy (XPS), Fourier transform infrared (FTIR) spectroscopy, solid-state nuclear magnetic resonance (NMR), and fluorescence spectroscopy are also discussed in this review for analyzing silica nanostructures. These

methods provide detailed insights into the structural and chemical properties of MSNs, enabling researchers to fine-tune their synthesis and functionalization processes.

This review aims to provide a comprehensive overview of the synthesis, characterization, and post-modification of MSNs and their diverse applications in the biomedical field. By highlighting recent advancements and ongoing challenges, it seeks to underscore the potential of MSNs in advancing healthcare technologies and improving patient outcomes.

2. SYNTHESIS OF MESOPOROUS SILICA NANOPARTICLES

2.1. Conventional Synthesis Methods

Mesoporous silica nanoparticles (MSNs) offer a promising drug delivery system and are extensively used in nanomedicine applications today [25]. The unique properties of silica nanoparticles are closely linked to their preparation process in the laboratory. Each treatment during the synthesis of silica nanoparticles results in variations in size and shape. This section describes a conventional method to synthesize MSNs with unique sizes and shapes.

According to the Stöber method [26], four key parameters influence the uniform size and shape of monodispersed silica nanoparticles, with diameters ranging from 50 nm to 2 μm: water, alcoholic solvent, ammonia, and alkoxysilane concentration. By adjusting these parameters, researchers can control the characteristics of the nanoparticles. Various agents, such as amines, alcohols, salts, and inorganic bases, affect the reaction rate during the hydrolysis and condensation of silica, which also regulates the particle size of MSN. In addition, investigating various parameters such as reaction temperature, concentration, and stirring rate also influences the particle size of the prepared MSN. In this context, Lv et al. [27] observed that the stirring rate significantly affects the particle size of MSNs. Furthermore, the concentration of reagents like triethanolamine (TEA) is essential in the particle size of MSN. TEA is used to stop particle growth and capture particle aggregation in MSN. Saputra et al. [28] studied the effect of alkoxysilane precursor, ethanol-to-water ratio, and the pH condition toward the size and shape of hollow mesoporous silica nanoparticles (HMSNs) optimized through Taguchi design of experiment (DoE). They found that those three parameters influence the size and shape of HMSNs and significantly affect the loading capacity of curcumin. Rahmani et al. [29] investigated the effect of alcohol concentration on the size and shape of MSN. They found that MSNs prepared with 20 μL mL^{-1} of ethanol had a monodispersed spherical nanostructure with a diameter of around 300 nm. However, when the ethanol concentration was increased to 100 μL mL^{-1}, the shape of the MSNs changed to nano-rods with diameters ranging from 450-600 nm. This demonstrates that the alcohol concentration can significantly influence the morphology of the silica nanoparticles. In addition to alcohol concentration, the choice of template surfactant also plays a crucial role in determining the size and shape of silica nanoparticles. Huang and co-workers explored the effects of combining two types of surfactants: cetyltrimethylammonium bromide (CTAB) and the commercially available surfactant Capstone FS-66 [30]. Their study revealed that adding Capstone FS-66 changed the MSN particle shape from a spherical nanostructure (obtained with only CTAB) to a dendritic-like structure. This is illustrated in Figure 1, where the morphological transformation is evident. Furthermore, the size of the nanoparticles increased with higher concentrations of Capstone FS-66. Specifically, the nanoparticle size became larger with the addition of this surfactant, indicating that the surfactant concentration is a critical factor in tailoring nanoparticle dimensions. However, the porous diameter of the nanoparticles was not controlled with the addition of 0.66 g of Capstone FS-66, suggesting that while surfactants can influence the overall size and shape, they may not necessarily allow for precise control over all structural aspects.

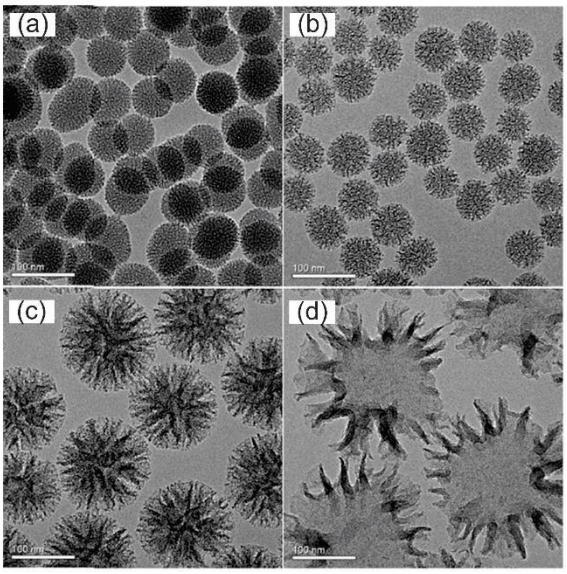

Figure 1. TEM images of MSN were prepared using (a) without and with (b) 0.15 g, (c) 0.32 g, and (d) 0.66 g of Capstone FS-66 added into 1.92 g CTAB. (Reused with permission from ref. [30], © 2017 American Chemical Society).

2.2. Advanced Synthesis Techniques

Substantial efforts have been made to advance the development of various techniques for synthesizing mesoporous silica nanoparticles (MSNs). Recent advancements include microwave-assisted synthesis, hydrothermal synthesis, ultrasonic-assisted synthesis, and the co-condensation method. Each technique offers a promising pathway for MSN preparation compared to traditional methods, as elaborated in Table 1. Compared to traditional methods, these advanced synthesis techniques offer improved control over the structural and functional properties of MSNs, making them highly suitable for a wide range of applications, including drug delivery, catalysis, and imaging. Briefly, the advanced synthesis approaches harness the power of cutting-edge techniques to prepare the MSNs. All the chemicals are like the conventional method, such as using alcoholic water as a solvent, base as a catalyst, and alkoxysilane as silica precursors. The main difference lies in the energy sources, which can significantly influence the hydrolysis and condensation during the formation of MSNs. Each technique offers advantages such as efficient synthesis time, energy consumption, product quality, control over physical and morphological properties, availability of additional functional groups, and more.

Energy-assisted approaches, particularly those involving microwave or ultrasound induction, have emerged as promising techniques for synthesizing MSNs. These methods leverage specific energy sources to drive chemical reactions more efficiently, enabling the formation of functional nanostructures with desirable properties [31, 32]. Microwave-assisted synthesis is a technique that uses microwave radiation, typically within the frequency range of 300 MHz to 300 GHz, to accelerate chemical reactions. The high-frequency electromagnetic waves generated in microwave-assisted synthesis cause polar molecules and ions in the reaction mixture to oscillate rapidly, generating heat through molecular friction. This localized heating significantly reduces the reaction time, often bringing it down to a matter of minutes or even seconds, compared to conventional heating methods, which may require hours. The efficiency in energy transfer allows for faster reaction kinetics, leading to the rapid formation of nanoparticles. As demonstrated by Mahalingam and Sivaraju [33], the preparation of MSNs through this method only takes 10 minutes, yielding a high amount of silica particles from the rice husk ash precursors with a diameter of 80-100 nm.

Ultrasound-assisted synthesis also offers unique advantages. Ultrasound waves, typically in the frequency range of 20 kHz to several MHz, create cavitation bubbles in the reaction mixture. The collapse of these bubbles generates localized high temperatures and pressures, which can drive the formation of nanoparticles like microwave-assisted synthesis. This method can be used to prepare MSNs as reported by Thongnoppakhun [34]. Typically, the reaction mixture comprising TEOS, a

solvent mixture of ethanol and water, and ammonium hydroxide catalyst was introduced into the chamber. To mitigate uncontrolled reactions resulting from the high localization energy of ultrasounds, the researchers employed an indirect ultrasound irradiation technique. Through this methodology, a hollow interior of MSNs was generated with a diameter of approximately 500 nm, which could be directly utilized to encapsulate curcumin within the hollow structure.

The hydrothermal method involves the use of water as a solvent under high temperature and pressure conditions within a sealed vessel, typically an autoclave. This method allows for precise control over the temperature and pressure, which directly influences the size, shape, and crystallinity of the nanoparticles. Sun et al. [35] successfully prepared highly monodispersed and large-pore MSNs by employing this method. They used sulfuric acid during the synthesis of MSNs to enlarge the pore size. Owing to their controlled particle size and large pore, the MSNs have high surface area exceeding 500 m^2/g which is further used to load water insoluble-drug indomethacin. In another report, Sun et al. [36] also prepared MSNs by the hydrothermal method. Instead of using sulfuric acid, currently, they employ $NaBH_4$ as an additive to precisely control the morphology of the MSNs. As a result, they effectively produced ultra-large mesopores of MSNs with a surface area of 1104 m^2/g.

TABLE I. The advantages offered by non-conventional methods in the synthesis of MSNs

Methods	Advantages	Ref.
Microwave-assisted synthesis	**Efficiency and Speed**: This technique significantly reduces synthesis time due to rapid and uniform heating. The energy-efficient process leads to well-controlled particle size and morphology. **Enhanced Properties**: MSNs produced via microwave-assisted synthesis often exhibit improved textural properties, such as higher surface area and pore volume, enhancing their application potential.	[37, 38]
Hydrothermal	**Crystalline Quality**: This method involves the crystallization of MSNs from high-temperature aqueous solutions at high pressures, leading to high-purity and highly crystalline nanoparticles. **Controlled Morphology**: Hydrothermal synthesis allows precise control over particle size and shape, which is crucial for applications requiring specific MSN geometries.	[39, 40]
Sonochemistry	**Enhanced Dispersion**: Ultrasound waves promote better dispersion of reactants, resulting in uniform particle size distribution. **Reduced Reaction Time**: The cavitation effect induced by ultrasonic waves accelerates chemical reactions, thereby reducing the overall synthesis time.	[41, 42]
Co-condensation	**Functionalization:** This method allows for the simultaneous incorporation of functional groups during the synthesis process, enabling the production of MSNs with tailored surface properties. **Versatility:** The co-condensation method can introduce various organic and inorganic components, enhancing the functional diversity of MSNs.	[43, 44]

2.3. Synthesis protocols for different types of MSNs

MCM-41 (Mobil Composition of Matter No. 41) is a mesoporous material belonging to the M41S family of materials developed by Mobil Oil Corporation researchers in the early 1990s [8]. It is characterized by its highly ordered hexagonal array of cylindrical mesopores, typically in the range of 2-10 nm in diameter, very high surface area exceeding 1000 m^2/g, and possesses a significant pore volume. The synthesis of MCM-41 typically involves a templating method using surfactants such as cetyltrimethylammonium bromide (CTAB) in an alkaline medium. The surfactant molecules form micelles that template the mesoporous structure. After forming the silica framework, the surfactant is removed by calcination or solvent extraction, leaving behind the porous structure. Recently, Aquino et al. [45] harnessed industrial sodium silicate as silica precursors in the synthesis of MCM-41 by following an advanced hydrothermal method. It involves CTAB as a template and H_2SO_4 as a catalyst in the formation of MCM-41, which is further hydrothermally treated for 4 h at 100 °C.

SBA-15 is a mesoporous silica material known for its large, well-ordered pores and thick pore walls. Developed by researchers at the University of California, Santa Barbara (hence the acronym SBA), SBA-15 has unique properties that make it suitable for a variety of applications [46-48]. The synthesis of SBA-15 involves using a block copolymer, such as Pluronic P123, as a structure-directing agent in an acidic medium. The copolymer forms micelles that template the formation of the mesoporous structure. After the silica framework forms around the micelles, the polymer is removed through calcination or solvent extraction, resulting in the mesoporous material. SBA-15 exhibits a highly ordered hexagonal array of cylindrical mesopores, similar to MCM-41, but with larger pore diameters and thicker walls. The pore sizes typically range from 5 to 30 nanometers, and the pore walls are significantly thicker, which provides enhanced thermal and mechanical stability.

KIT-6 is a mesoporous silica material known for its three-dimensional (3D) cubic pore Ia3d structure. Developed by researchers at the Korean Institute of Technology (hence the acronym KIT), KIT-6 possesses a high surface area, usually between 700 and 1000 m^2/g, with pore diameters ranging from 5 to 10 nm. This combination of large pores and high surface area enhances its capacity for hosting large molecules and facilitates efficient diffusion [49, 50]. The synthesis of KIT-6 involves using a structure-directing agent, such as a block copolymer (e.g., Pluronic P123), in the presence of a co-surfactant (e.g., n-butanol) under acidic conditions. The mixture forms a bicontinuous microemulsion that templates the formation of the 3D cubic mesostructured. After the silica framework forms around the micelles, the surfactants are removed through calcination or solvent extraction.

Hollow MSNs (HMSNs) are made using various synthetic methods because the interstitial space within these MSNs is empty, allowing for ample bioactive accommodation space due to mesopores in the outer shell. Hollow MSNs have a large surface area, high pore volume, and controlled release behavior (due to mesoporous shell channels) [51]. Because of the larger cavity volume, the drug loading capacity of hollow mesoporous silica nanoparticles (hollow MSNs) is greatly improved, allowing for an enormous amount of drug loading compared to solid MSNs, which have restricted volumes. This increasing volume has a direct impact on the drug-loading area [52]. Hollow MSNs can be synthesized using hard or soft template methods, spray drying, and selective etching techniques [53]. The hard template technique involves producing mesoporous material or solid nanocrystals in situ with pore wall diameters ranging from 2 to 50 nm. Various materials such as TiO_2, SnO_2, Cu_2O, Fe_2O_3, Ag, Pt, and polymer beads have been investigated for colloidal hard templating methods. With "polymer latex particles" such as polystyrene (PS) and polymethylmethacrylate (PMMA), it is simple to produce hollow MSNs. These particles have various sizes, which are affordable, homogeneous, and easily removed by calcination at 300 - 500 °C. In contrast, expensive inorganic colloids must be eliminated using an acid solution, complicating the synthesis [54]. In the soft templating method, amphiphilic surfactants that can self-assemble and form micellar aggregates and oil-in-water systems are utilized [55]. Amphiphilic molecules with hydrophilic and hydrophobic properties, such as micelles, emulsions, bubbles, and vesicles, serve as templates in the soft template method. The material is then deposited and solidified onto the template, and the template is eliminated through calcination or extraction to create a porous material [52]. This method offers several advantages over other chemical methods for producing hollow MSNs, such as greater control over the synthesis process, lower production cost, a broader range of multifunctional capabilities, and higher variability than MSNs with a hard template [52, 56]. A common approach for producing hollow MSNs is using a dual template approach with a hard template to make a hollow core and a soft template as a pore-forming agent to construct mesopores in the shell. A mixture of hydrophobic silane and organic silica sources (such as TEOS) is required for the one-pot production of silane-containing hollow MSNs. The newly hydrophilic TEOS and silane sources spread and co-condense on the surface of the microemulsion to form solid hollow MSNs following hydrolysis [54]. When solid hollow MSNs are formed, the templates can be eliminated using thermal calcination or solvent extraction [57].

3. CHARACTERIZATION OF MESOPOROUS SILICA NANOPARTICLES

3.1. Structural Characterization

In 1992, Beck and co-worker [10], a researcher from Mobil Research and Development Corporation, successfully synthesized a new family of molecular sieves called MCM-41 prepared by liquid crystal template according to the schematic pathway described in Figure 2a. From several characterizations, this new class of silicate mesoporous molecular sieves was claimed to have a hexagonal arrangement of uniform mesoporous with dimensions between ~15 Å to greater than 100 Å. The organic template, also called a liquid crystal surfactant, played an essential role in the silica nanostructure direction, causing a high surface area above 700 m^2/g with a large pore volume of hydrocarbon sorption by 0.7 cc/g. Figure 2b demonstrated an X-ray powder diffraction pattern of calcined MCM-41, typically observing four peaks, a characteristic of MCM-41, indexed as a hexagonal lattice. Remarkably, it has a hexagonal morphological structure observed by TEM in Figure 2c.

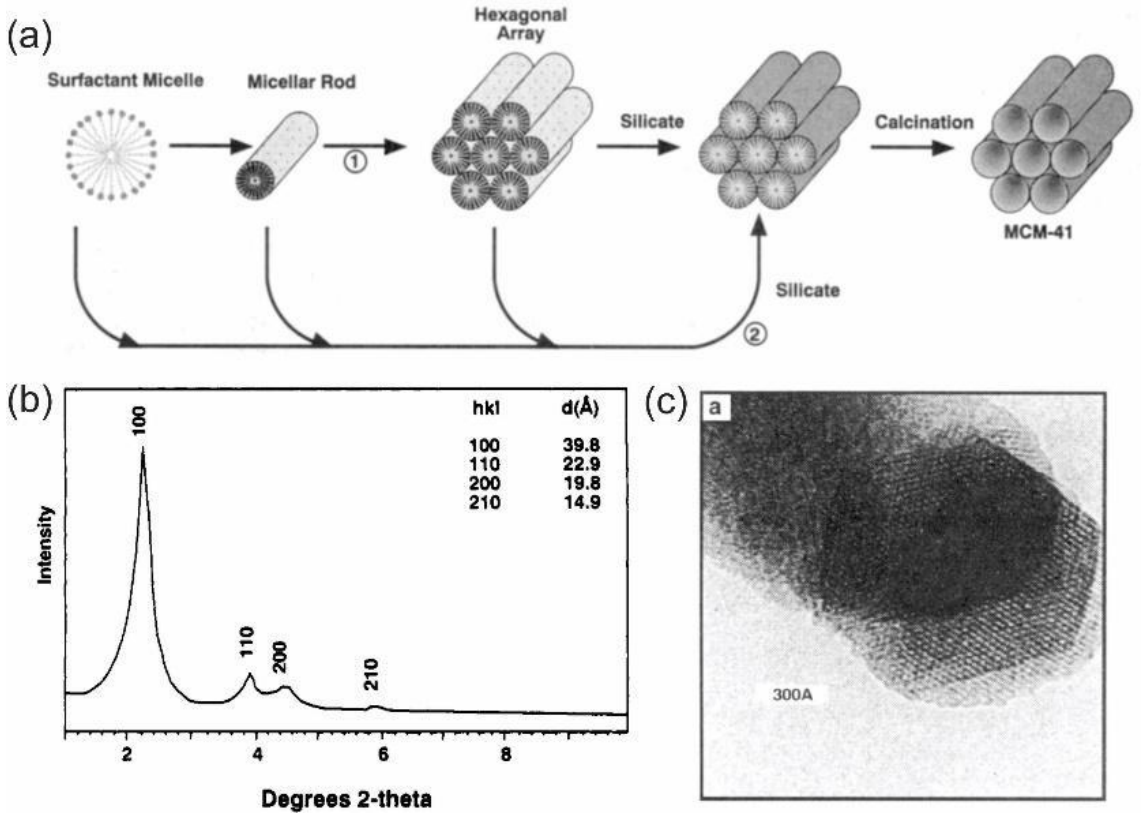

Figure 2. (a) Schematic pathway to synthesize MCM-41. (b) XRD pattern of calcined MCM-41. (c) TEM image of MCM-41. (Reuse with permission from ref. [10], © 1992 American Chemical Society)

Three-dimensional hexagonal mesoporous silica, SBA-2, was first introduced in 1995, motivated by the previous achievement of successfully synthesizing ordered mesoporous silica, well known as MCM-41 [12]. This nanostructure was dimensionally tailored by incorporating a novel surfactant containing two quaternary ammonium groups attached to the hydrophobic tail, namely Gemini surfactant, with a mesostructure analogue with a zeolite cage structure. The XRD pattern of calcined and as-made BSA-2 revealed that the BSA-2 could be indexed in (100), (002), (101), (110), (103), (112), and (211) for calcined BSA-2 and additional peak at (004), (300), (302), (220), and (310) for as-made BSA-2, both of them assigned as $P6_3/mmc$ space group with lattice ratio by c/a = 1.61 to 1.63.

Novel mesoporous silica noted as SBA-16 was successfully prepared by Zhao and co-workers [11] using a narrow concentration of poly(alkylene oxide) triblock co-polymer $EO_{106}PO_{70}EO_{106}$ as an organic template at room temperature under acidic condition for 20 h. Figure 3 shows an X-ray

powder diffraction pattern of as-synthesized and calcined SBA-16 having strong reflection in 2θ under 1° with *d* spacing by 124 Å and more weak reflection observed at 2θ above 1°. The X-ray powder diffraction of calcined SBA-15 was reflected as cubic structure (*Im3hm* space group, *a*= 166 Å) with hkl index by (110), (200), (211), (220), (310), (222), and (321).

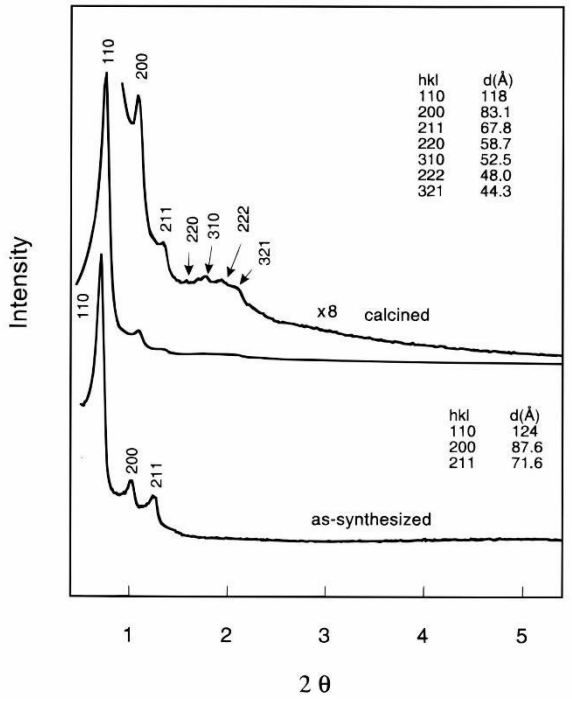

Figure 3. XRD pattern of SBA-16. (Reuse with permission from ref. [11], © 1998 American Chemical Society)

Highly ordered and novel mesoporous silica templated by spheric form surfactant containing a rigid unit of the hydrophobic chain was magnificently achieved in 1999 by Zhao and co-worker, [13] denoted as SBA-8. This silica mesophase is thermally stable in the air and has a high surface area above 1000 m^2/g. The dimensional structure of SBA-8 is two-dimensional rectangular and can be indexed in the space group *cmm* with lattice parameter $a/b < \sqrt{3}$ obtained from the X-ray powder diffraction pattern in Figure 4a. After template removal by calcination at 500-600 °C, the 110 and 200 reflections were shifted compared to the as-made SBA-8. The strong reflection is observed at 110 and 200 index; meanwhile, weak reflection was observed at 2θ range of 4-6.5°. Figure 4b reveals the cell parameter differences between SBA-8 and MCM-41 (space group *p6mm*). The elongation of the hexagonal channel and shrinkage occur along the *b* and *a* direction, respectively, found in the SBA-8 cell structure.

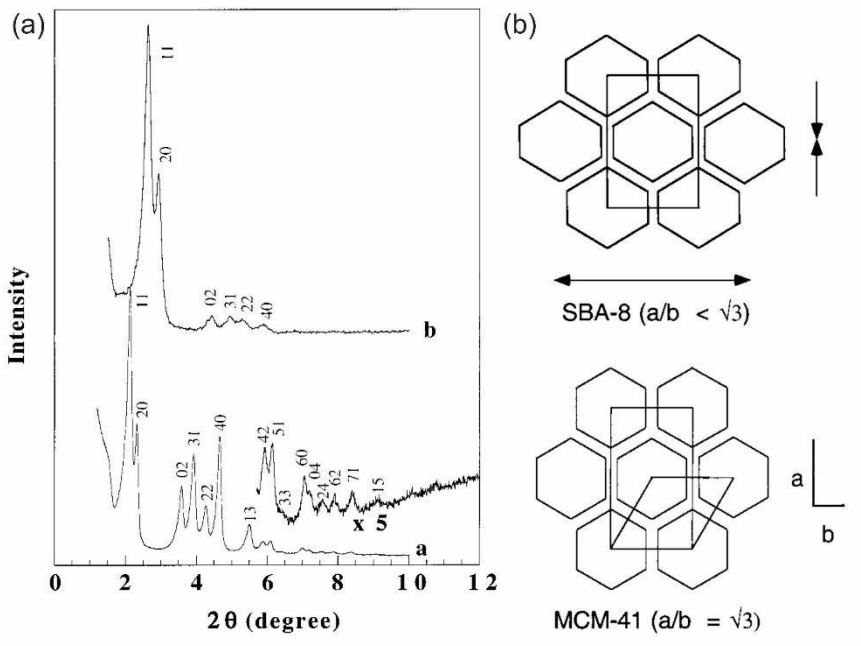

Figure 4. (a) XRD pattern of a. as made and b. calcined SBA-8. (b) Structural dimension comparison between SBA-8 and MCM-41. (Reuse with permission from ref. [13], © 1999 American Chemical Society).

The disordered channel structure of MSNs was synthesized using tetraethylorthosilicate templated by nonionic surfactant (polyethylene oxide) reported in 1995 by a researcher from Michigan State University [14]. The product of this first trial was then branded as MSU-1. The x-ray powder diffraction pattern of as-synthesized and calcined MSU-1 displays only a broad peak at *d* basal spacing 4.6 nm for as-synthesized MSU-1 and 4.1 nm for calcined MSU-1. Not only did the *d* basal spacing shift, but the intensity was dramatically increased, as observed in the XRD data, indicating the ordering improvement of the oxide framework. TEM characterization proved the disorder channel structure. The TEM image showed that the MSN structure lacks long-range packing order. Consequently, it defects the channel assembly, forming cylindrical- to hexagonal-shaped channels.

3.2. Surface and Chemical Characterization

To evaluate the surface interaction between the grafting compound and silica nanoparticles, X-ray photoelectron spectroscopy (XPS) was introduced. Evaluation of nanoparticle chemistry, especially surface chemistry, has raised concern since it is crucial information related to both the application and nanoparticle processing, as well as to point out the nanoparticle interaction with the surrounding environment [58]. The XPS data provides information concerning material surfaces' quantitative elemental and chemical states [59]. This technique was combined with time-of-flight secondary ion mass spectrometry (ToF-SIMS) to offer more information about chemical and molecular structure by generating mass data of substrates or even chemical species in low concentration. The data delivered by ToF-SIMS confirms that the organic fragments have a positive or negative charge. Ambrogio et al. [60] utilized this combination technique to analyze the organic substrates, in this case β-Cyclodextrin, grafted on silica nanoparticle surfaces (see Figure 5a). The survey scan of β-Cyclodextrin grafted silica nanoparticles is shown in Figure 5b. The data provided little information on the interaction between silica surfaces and β-cyclodextrin. An exciting investigation was obtained after scanning and fitting the XPS spectra at a narrow range between 290-282 eV to gain detailed information on structural and binding energy relating to the carbon atom (Figure 5c). The signal intensity of the peak at 288 eV was a significant increase occasioned by the large number of C-O generated from the 1,4-glycosidic bond of β-Cyclodextrin. The carbon-to-silicon ratio was also measured from XPS, earning 1.54. Additionally, the ToF-SIMS spectra in Figure 5d confirmed the presence of β-Cyclodextrin compounds on silica surfaces, as indicated by

fragments at 142, 184, and 242 amu. The results proved that β-Cyclodextrin is attached to the silica surfaces.

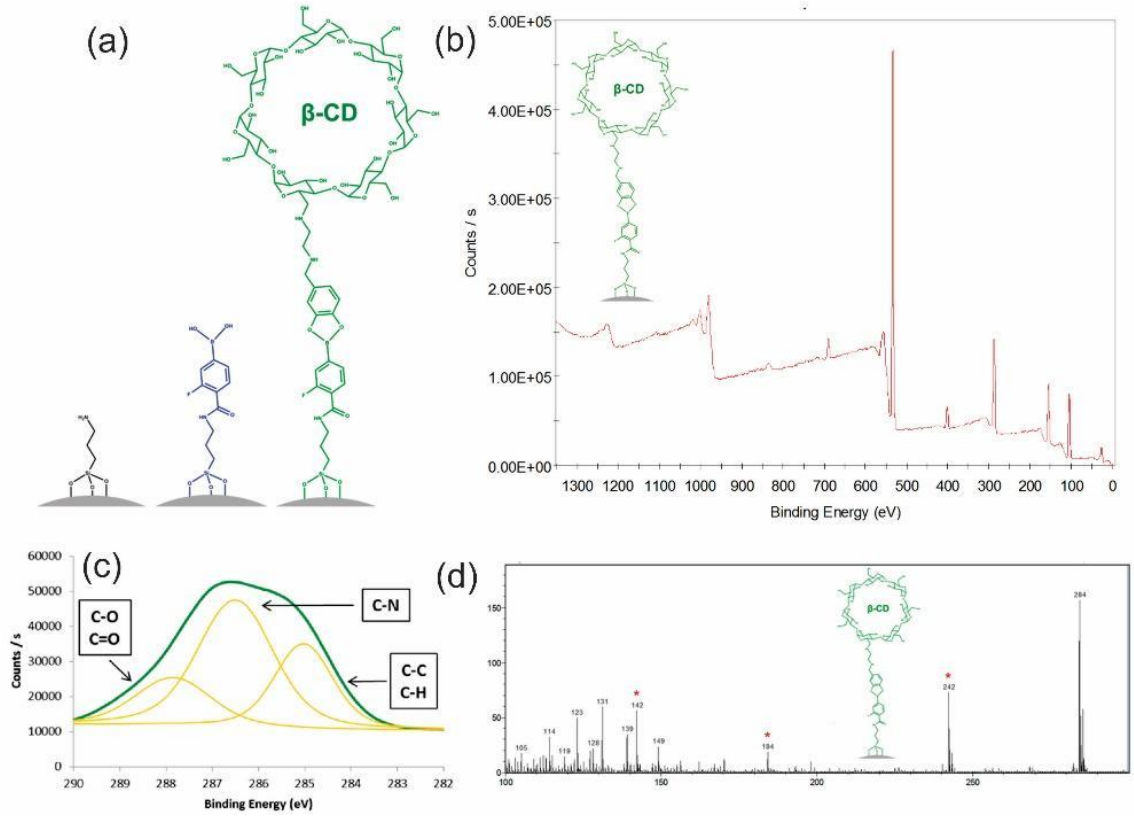

Figure 5. (a) Representative of molecular structure attached to nanoparticle surfaces. (b) XPS spectra of β-Cyclodextrin grafted silica nanoparticles. (c) XPS carbon narrow scan. (d) ToF-SIMS spectra of β-Cyclodextrin grafted silica nanoparticles. (Reuse with permission from ref. [60], © 2013 American Chemical Society).

Hartono et al. [61] functionalized the mesoporous silica nanoparticle with degradable poly(2-dimethylamino ethyl acrylate) (PDMAEA), termed PDMAEA-LPMSN, as gene nanocarrier, where the schematic synthesis is shown in Figure 6a. This nanostructure was designed as follows: First, the synthesized silica nanoparticle using fluorocarbon surfactant was functionalized by an alkoxysilane compound containing an azide group derived from 3-aminopropyltriethoxysilane (APTS) through a two-step reaction. Afterwards, fluorocarbon surfactant was removed from the azide-silica nanoparticle (signed as A-MSN), leaving a large cavity of about 11 nm and a high surface area of approximately 400 m^2 g^{-1}. In the third step, the chloroquine was loaded into nanoparticles, and subsequently, the PDMAEA was attached to the A-MSN by click chemistry to prevent the chloroquine's premature release. This formation is relatively easy to achieve since the PDMAEA has an alkyne group that interacts with the azide group of A-MSN. The fifth step was the loading of siRNA, and after hydrolysis, siRNA and chloroquine were released. Evaluation of chemical binding between organic functional compounds with MSNs and elemental composition was performed using XPS; the result is shown in Figure 6b for A-MSN and Figure 6c for PDMAEA-LPMSN. The data revealed that after introducing an alkoxysilane compound containing an azide group, the percentage of nitrogen atoms was 1.33% and increased to 5.12 when PDMAEA attached it. Before being modified with PDMAEA, two N peaks were observed in XPS spectra of A-MSN assigned as N1 and N2 represented as N^- and N^+ species typical of the azide group. However, by hosting PDMAEA, only one N peak was perceived, indicating the successful reaction between the azide and alkyne groups. Consequently, one C-N signal was found instead of two signals of the typical azide group. A similar result was also achieved by Chen et al. [62] in the modification of silica nanoparticles with unique polymer behavior, poly(N-isopropyl acrylamide) (PNIPAM). The characteristic peaks of the azide

group appeared at 399.8 eV and 403.9 eV were reduced to a single peak after attaching PNIPAM by click chemistry, viz. 400.1 eV. It evidenced that the azide group was completely transformed into a 1,2,3-triazole unit attached to the propargyl group of PNIPAM.

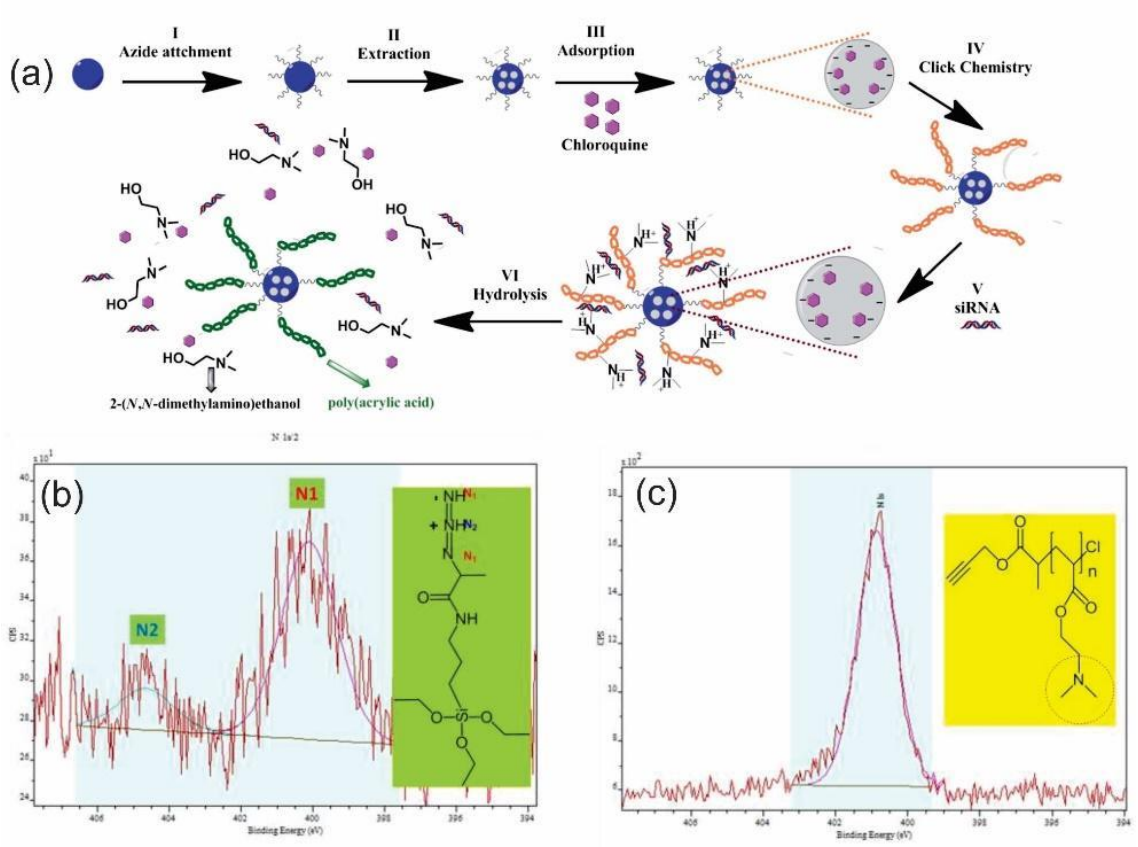

Figure 6. (a) Illustration of chloroquine loading and siRNA binding to LPMSNs. High-resolution XPS spectra of (b) A-MSN and (c) PDMAEA-LPMSN. (Reuse with permission from ref. [61], © 2014 The Royal Society of Chemistry).

FTIR and NMR spectroscopies are other essential tools for analyzing and characterizing the silica nanoparticle and its modification. Generally, FTIR and NMR spectroscopies are used to identify functional groups, point out the chemical structure, and determine the interaction of substances seen from the shift of wavenumber for FTIR and chemical shift for NMR. In silica nanostructure design, both spectroscopies are often employed to evaluate the successfulness of functionalization. For example, the functionalization of silica nanoparticles (diameter 13 nm) grafted by alkoxyamine and poly(styrene) was characterized with FTIR and ^{29}Si- and ^{13}C- CP/MAS solid-state NMR [63]. Poly (styrene)-grafted silica was prepared through two stages, as represented in Figure 7a—first, the functionalization of silica surface by alkoxyamine-based *N*-tert-butyl-*N*-(1-diethylphosphono-2,2-dimethylpropyl) nitroxide (DEPN). In the second stage, poly(styrene) is formed on the silica surface by adding a styrene compound initiated by a free sacrifial alkoxyamine compound. Each stage of this process was characterized using FTIR, reported in Figure 7b. Typically, the silica has three characteristic vibration bands: ν O-H, δ O-H, and ν O-H.

However, some peaks appeared after alkoxyamine was grafted onto silica nanoparticles. The peaks were characteristic of carbonyl vibration (ν C=O, 1734 cm^{-1}) and the aliphatic groups (ν C-H, 2850, 2920, and 2980 cm^{-1}; δ C-H, 1384 cm-1). The vibration of the aromatic polystyrene ring was observed in IR spectra of poly(styrene)-grafted silica, which appeared at 1450-1600 cm^{-1}. All of the data supported the grafting formation of poly(styrene) onto silica and alkoxyamine either. More complex analysis to strongly prove the chemical grafting of alkoxyamine onto silica was performed using ^{29}Si- and ^{13}C- CP/MAS solid-state NMR shown in Figure 7c and 8d, respectively. Three dominant signals appeared in ^{29}Si-NMR, i.e., -109.0 ppm, -101 ppm, and -58 ppm, allocated as Q^4,

Q^3, and T^2 signals, respectively. Both Q^4 and Q^3 signals were attributed as typical peaks of silicon atom framework [Si(4OSi)] and surface silanol group [Si(3OSi, 1OH)]. However, a broad T^2 signal corresponded to [Si(2OSi, 1R, 1OR′] species. The presence of the T^2 signal proved that the grafting of alkoxyamine was successfully achieved. ^{13}C-NMR carried out further investigation, shown in Figure 7d, supporting the result confirmed by ^{29}Si-NMR.

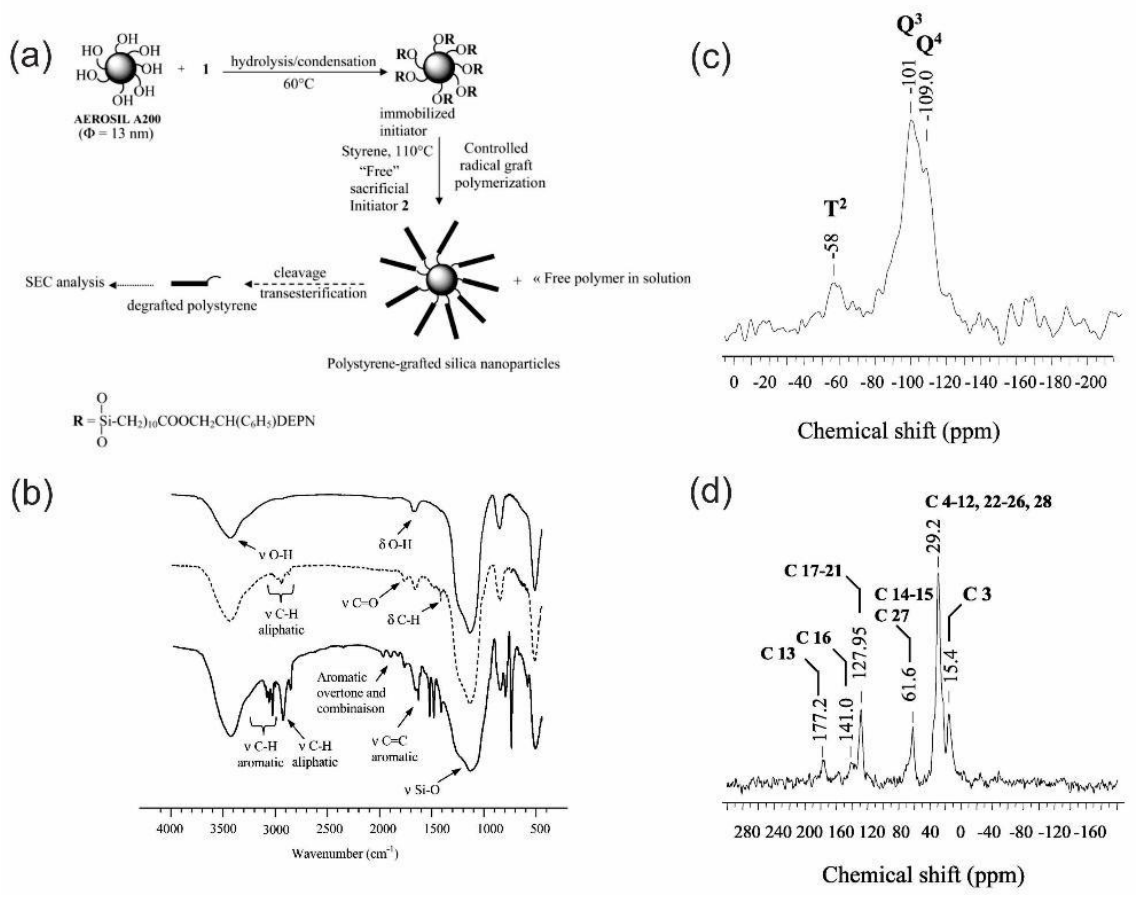

Figure 7. (a) Grafting schematic illustration. (b) IR spectra of silica nanoparticle (upper), alkoxyamine-grafted silica (middle), and poly(styrene)-grafted silica (bottom). (c) ^{29}Si- and (d) ^{13}C-CP/MAS solid-state NMR spectra of alkoxyamine-grafted silica. (Reuse with permission from ref. [63], © 2003 American Chemical Society)

4. BIOMEDICAL APPLICATION OF MSNs

4.1. Application of MSN in bioimaging

In medicine, silica nanoparticles have been labeled with biocompatible dye molecules for diagnostic purposes, resulting in fluorescence moieties in solutions analyzed by fluorescence correlation spectroscopy (FCS) [64]. This technique also assesses the concentration, brightness, and monodispersity of fluorescence probes related to the utility of nanoparticles. Ow et al. [65] employed this method to characterize the fluorescent properties of core-shell dye-labeled silica nanostructures synthesized through a two-stage reaction, as illustrated in Figure 8a. In the first stage, organic dye molecules were condensed and conjugated with silica precursor, resulting in a dye core. In the second stage, additional silica monomers were added, creating a denser silica network covering the dye core. The researchers used different organic dye-labeled compounds to produce core-shell fluorescent silica nanoparticles with varying UV-vis adsorption and emission responses, as shown in Figure 8b. Another investigation of fluorescent spectroscopy utilization was conducted by Prasad and co-workers [66], who explored the fluorescent properties of silica nanoparticles for gene delivery and their optical monitoring of intercellular transfer. They found that high monodispersity fluorescent dye-encapsulated silica nanoparticles exhibit high stability in aqueous suspension and effectively

protect DNA against enzymatic digestion, allowing for the formation of an excellent complex structure.

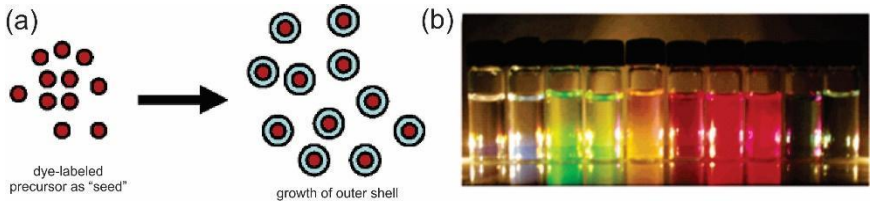

Figure 8. (a) Schematic representation of the synthesis of core-shell fluorescent silica nanoparticles. (b) UV-vis absorption and emission responses of different organic dyes covered by silica, from left to right, are Alexa 350, N-(7-(dimethylamino)-4-methylcoumarin-3-yl), Alexa 488, fluorescein isothiocyanate, tetramethylrhodamine isothiocyanate, Alexa 555, Alexa 568, Texas Red, Alexa 680, and Alexa 750. (Reuse with permission from ref. [65], © 2005 American Chemical Society).

Wiesner and co-worker [67] utilized the Modified Stöber method to develop core-shell fluorescent silica nanostructures using two dyes: fluorescein isothiocyanate (FTIC) as the sensor dye and tetramethylrhodamine isothiocyanate (TRITC) as the reference dye (illustrated in Figure 9a). The combination of these dye molecules covalently bonded to the silica shell aimed to enhance particle brightness and simplify particle tracking. The nanoparticle with the desired core size was characterized using spectrofluorometry and tested in various pH buffer solutions ranging from 5 to 8.5, as shown in Figure 9b. The results demonstrated that the photoluminescence intensity of core-shell fluorescent silica nanoparticles in different pH buffer solutions varied, with the highest intensity observed at high pH. This finding confirmed the pH-dependent quantum efficiency adjustment revealed by fluorescein in conjunction with tetramethylrhodamine as an internal standard (Figure 9b). To evaluate the sensing capabilities of the core-shell fluorescent silica nanoparticles embedded in rat basophilic leukemia mast cells (RBL-2H3), an in vivo test monitored by confocal microscopy, as shown in Figure 9c, was performed. By incorporating TRITC and FTIC as reference and sensor dyes, the researchers enhanced the detection of silica in RBL mast cells. They discovered that the various intracellular compartments had pH values ranging from pH 6.5, indicative of early endosomes, to pH ~5.0.

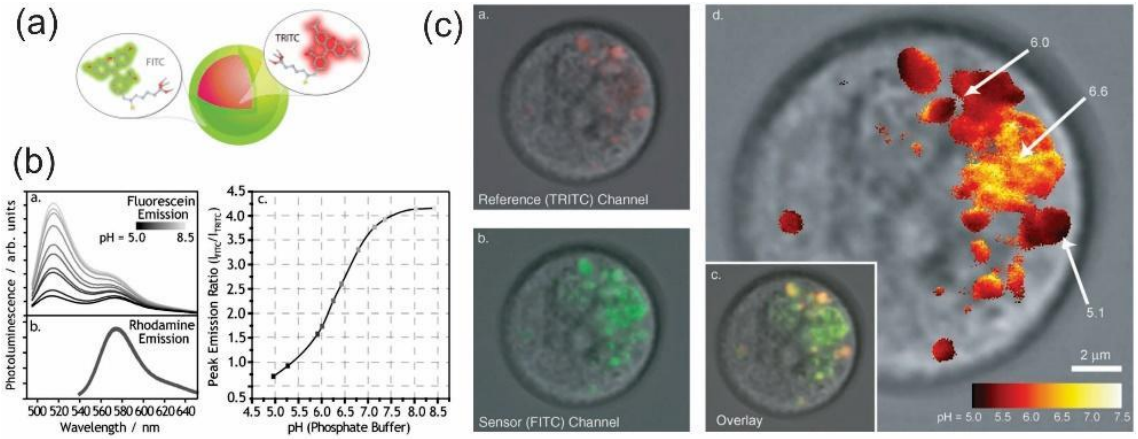

Figure 9. (a) Diagram of core/shell fluorescent silica nanostructure. (b) Spectrofluorometric analysis of the nanoparticle for pH sensing; a. fluorescence spectra at various pH levels, b. reference tetramethylrhodamine emission spectra, c. ratiometric calibration curve. (c) Confocal fluorescence imagery of a. TRITC dye, b. FTIC dye, c. composite image, d. false-color ratiometric imaging in cellular compartments. (Reuse with permission from ref. [67], © 2006 Wiley-VCH Verlag GmbH & Co. KGaA, D-69451 Weinheim).

A novel class of fluorescent dye molecule, 9,10-bis[4′-(4″-aminostyryl)styryl]anthracene (BDSA), was prepared as a two-photon energy donor in silica nanoparticles combined with a

photosensitizer energy acceptor, 2-devinyl-2-(1-hexyloxyethyl)pyropheophorbide (HPPH) [68]. Figure 10a displays the optimized geometry structure of the BDSA molecule, while Figure 10b shows the fluorescence spectra of HPPH-loaded silica nanoparticles with different amounts of BDSA (10 and 20 wt %). The fluorescence dramatically improved after incorporating 10 wt % and 20 wt % of BDSA due to an efficient up-conversion of near-IR light energy to excite HPPH by BDSA aggregates. The in vitro assessment was carried out to evaluate the potential of the HPPA/BDSA encapsulating silica nanoparticle as a drug carrier against HeLa cells under two-photon excitation at 850 nm. Figure 10c shows the fluorescence imaging of HeLa cells cured with the nanoparticle containing 1.1 wt % of HPPH and 20 wt % of BDSA, taken by two-photon laser scanning microscopy. The tumor cells actively uptake the encapsulating nanoparticle, as observed from the fluorescence imaging, giving an intense fluorescence signal. Moreover, the intercellular stability of the HPPH/BDSA encapsulating silica nanoparticles was observed and proven by the intercellular FRET (fluorescence resonance energy transfer), which is still operating in the cellular environment. The result showed that the presence of both HPPH and BDSA was potential for cancer photodynamic therapy (PDT). PDT is a promising treatment alternative to either chemotherapy or radiotherapy for cancer therapy, as it works by activating photosensitizer drugs at a specific wavelength to significantly yield cytotoxic reactive oxygen, executing cell death as a result of an energy transfer [69, 70].

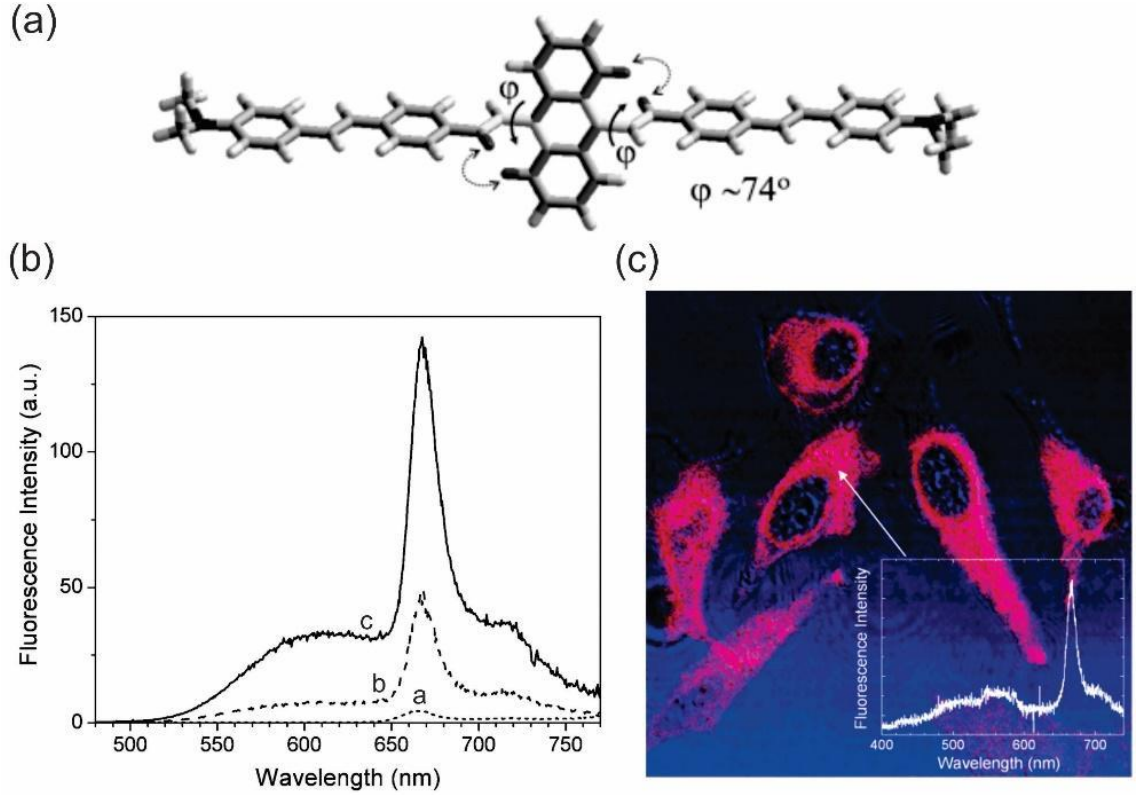

Figure 10. (a) Geometrically optimized BDSA structure. (b) Fluorescence spectra of silica nanoparticle entrapping a. 1.1 wt % HPPH, b. 1.1 wt% HPPH/10 wt % BDSA, c.1.1 wt % HPPH/20 wt % BDSA. (c) The transmission (blue) and two-photon excited fluorescence (Red) image of HeLa cells. (Reuse with permission from ref. [68], © 2007 American Chemical Society).

Another study by Bagwe et al. [71] utilized an inorganic-based labeled dye to fabricate fluorescence silica nanoparticles. Specifically, the researchers employed tris(2,2′-bipyridyl)dichlororuthenium(II), also known as Ru(bpy) (refer to Figure 11a), which was doped into silica nanoparticles to yield high fluorescence intensity at 594 nm when the nanoparticles were prepared in a dual oil/water emulsion with water: surfactant ratio of 5. While the nanoparticles synthesized in the dual oil template consisting of Triton X-100 and cyclohexane, as well as the hexanol system aided by 1.5% ammonium hydroxide, exhibited lower fluorescence intensity at 8.7

x 106, they had a smaller particle size of 52 nm and 178 nm for the silica nanoparticles prepared in the oil/water system. In contrast, the silica nanoparticles synthesized in the oil/hexanol system exhibited a more uniform particle size distribution and a spherical morphological shape, as depicted in Figure 11b.

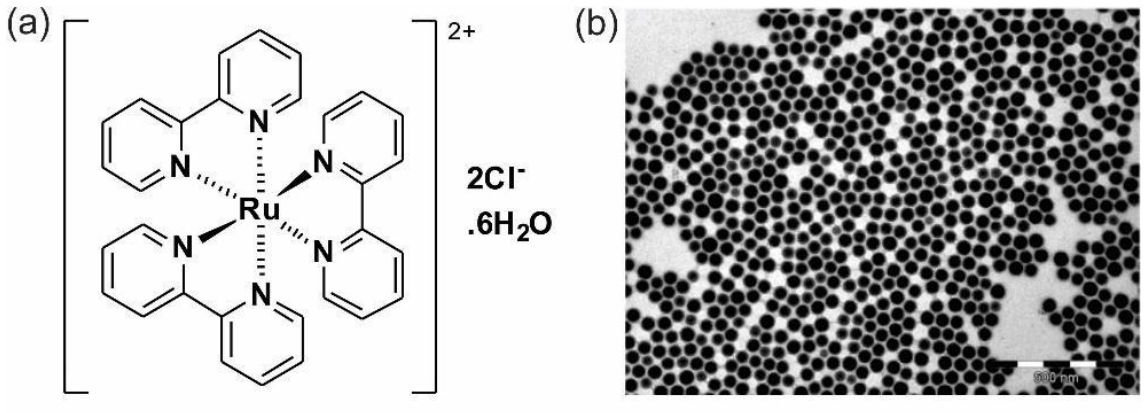

Figure 11. (a) Tris(2,2′-bipyridyl)dichlororuthenium(II) chemical structure. (b) TEM image of Ru(bpy) dye-doped silica nanoparticle prepared in oil/hexanol aided by 1.5% ammonium hydroxide. (Reuse with permission from ref. [71], © 2004 American Chemical Society).

4.2. Application of MSNs as drug delivery

Due to their highly porous structure and flexibility in surface modification, MSNs have become increasingly popular as drug delivery systems in recent years. These characteristics make MSNs exceptionally versatile, allowing them to be engineered for various biomedical applications. As shown in Figure 12, MSNs can be engineered to serve as effective nano-drug delivery platforms, offering several key advantages: (1) the surface and morphology can be fine-tuned to ensure the biocompatibility and safety of the drug carrier. One of the primary benefits of MSNs is the ability to fine-tune their surface properties and morphology. By adjusting factors such as pore size, shape, and surface charge, MSNs can be designed to enhance their biocompatibility, ensuring that the drug carrier is safe for use in biological systems. This customization also allows for the optimization of drug loading capacity and release profiles, minimizing potential side effects and improving the therapeutic efficacy of the drug; (2) The nanostructure of MSNs can be specifically engineered to allow for controlled drug release. This can be achieved by designing the MSNs to respond to various internal stimuli (such as pH, redox conditions, or enzymes) or external stimuli (such as temperature, light, or magnetic fields). For example, in a tumor microenvironment where the pH is lower than in healthy tissue, MSNs can be designed to release their payload more readily, thereby targeting the drug delivery to cancer cells while sparing healthy tissues. This ability to control drug release in response to specific stimuli not only enhances the efficacy of the treatment but also reduces the risk of premature drug release, which can lead to toxicity and other side effects; (3) The surface of MSNs is rich in hydroxyl groups, which provide numerous sites for chemical modification. By conjugating small molecules, polymers, peptides, proteins, or antibodies to these hydroxyl groups, researchers can improve the retention of drugs within the pores of the MSNs, preventing premature release. Additionally, these modifications can enhance the cellular uptake of the MSNs, ensuring that the drug-loaded nanoparticles are efficiently absorbed by target cells. Furthermore, by attaching targeting ligands such as antibodies or peptides, MSNs can be directed specifically to diseased cells, improving the specificity of drug delivery and minimizing the impact on healthy tissues. By carefully designing and modifying the surface properties, researchers can create MSN-based systems that offer precise control over drug release, targeted delivery to specific cells, and enhanced therapeutic efficacy, ultimately leading to more effective and safer treatments for various diseases.

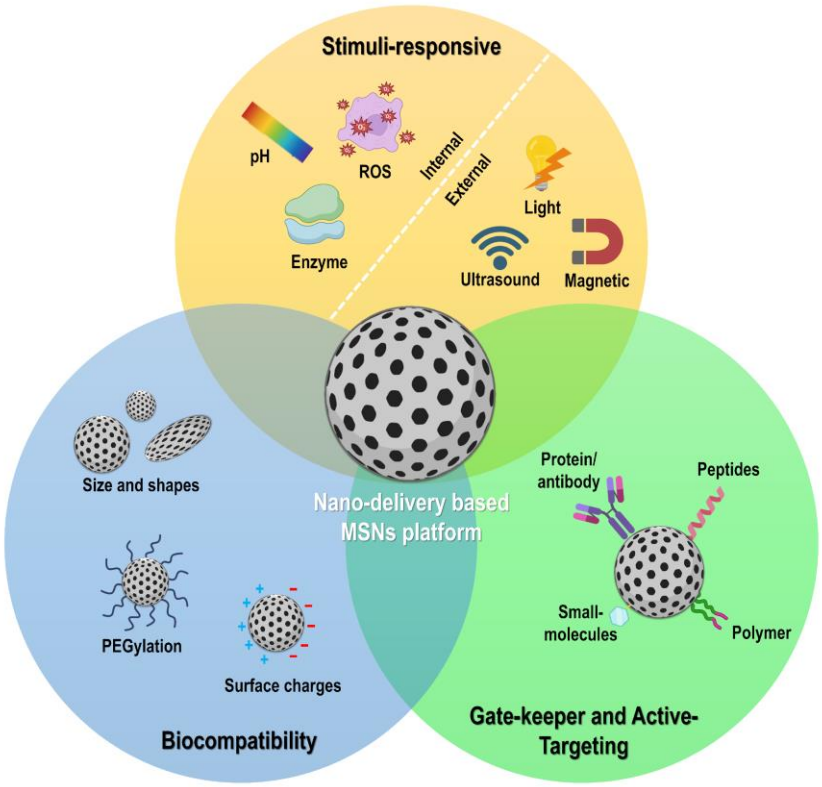

Figure 12. Characteristics of MSNs as potential nano-drug delivery platform.

By optimizing the nanostructure and surface functionalities, MSNs can effectively prevent the early release of cytotoxic drugs and enable the controlled release of therapeutics in response to internal or external triggers [72-75]. For example, redox-responsive drug carriers represent an alternative strategy for designing MSN nano-delivery systems, as cancer cell environments exhibit elevated levels of glutathione (GSH). Li et al. demonstrated that MSNs conjugated with 5-mercapto-2 nitrobenzoic acid (MNBA) via a disulfide linker exhibit a redox-responsive release mechanism, using the linker to block the pore channels in the presence of Doxorubicin (DOX). Wang et al. [76] molecularly engineered the framework of MSNs using a co-condensation method to create redox-responsive MSNs. In their study, they utilized two types of silica precursors, TEOS and bis-[gamma-(triethoxylsilicon)propyl]-tetra-sulfide (BTEPS), to incorporate a disulfide linker within the MSNs framework. The structurally modified MSNs are degradable in the presence of GSH, which can facilitate controlled drug release. The design of degradable MSNs was also successfully demonstrated by Yang et al. [77]. Their approach chemically engineered the silica framework by incorporating organic moieties containing disulfide bonds. As a result, the MSNs underwent degradation upon GSH exposure, which induced the release of DOX as a drug model. This controlled release mechanism enhanced the anticancer activity of the DOX-loaded MSN. A similar approach was reported by Hu et al. [78], who designed a degradable MSN composed of a tetrasulfide-organo linker within the silica framework and coated with polydopamine (PDA). Under redox stimuli, this nanoparticle released DOX through a nanoparticle degradation mechanism, and by incorporating an 808 nm laser, the PDA could enhance the anticancer activity through a photothermal mechanism. This synergistic photo-chemo therapy effectively suppressed tumor size in the mouse model.

Since the pH of the cancer microenvironment (approximately pH 4.5–6.5) is typically lower than that of healthy cells [79], the design of pH-responsive MSN drug carrier also becomes a promising approach. Our team recently developed a system using zwitterion-like small molecules, 4-((2-aminoethyl) amino)-4-oxobut-2-enoic acid (AmEA), conjugated to the surface of MSNs to control drug release triggered by pH [3]. Surface modification of MSNs by coating with chitosan polymer was reported to have pH-responsive drug release since this polymer is sensitive to pH [80], [81]. Previously, we harnessed the chitosan to coat the silica-encapsulated nanoemulsion surfaces to achieve pH-triggered curcumin release [4]. In another report, chemical conjugation of chitosan into

MSNs surfaces *via* oxirane linker resulted in a significant reduction (~19%) in curcumin release under physiological conditions [82]. A similar strategy using the oxirane linker to conjugate chitosan to MSNs was also applied for DOX delivery in breast cancer treatment [83]. The study found that incorporating chitosan on the surface of MSNs not only enabled pH-responsive drug release but also enhanced cellular uptake and endo/lysosomal escape of the nanocarrier, leading to improved therapeutic outcomes. Chen et al. [84] reported the successful development of MEMSNs, which are multifunctional envelope-type mesoporous silica nanoparticles synthesized by incorporating ultra-small lanthanide-doped nanoparticles ($NaGdF_4$:Yb/Tm@$NaGdF_4$) and ultra-thin TaO_x layer (S-NPs). The results indicated that the nanoparticle had the potential to act as a biocompatible and controllable drug carrier, as well as a magnetic resonance imaging (MRI) agent. While the high surface area of the nanoparticle was slightly decreased after being doped with S-NPs because of the pore-blocking effect, the S-NPs doped mesoporous silica (MS@S-NPs) demonstrated greater resistance to premature drug release in physiological environments compared to unmodified MS. Doxorubicin (DOX) was used as a drug guest molecule. It was quickly released from MS@S-NPs in an acid environment caused by the hydrolysis of acid-labile acetal at acidic conditions. Consequently, the gatekeeper or S-NPs was removed from the MS pore channel, allowing the DOX guest molecules to escape from the MS system at low pH. The cumulative drug molecule release was initially controlled at pH 7.4 but dramatically increased at pH 2 and 5. Since the MS has no gatekeeper, the cumulative drug release both in pH 7.4 and pH 5.0 was similar.

5. FUTURE PERSPECTIVES AND CHALLENGES

The development of MSNs with stimuli-responsive release mechanisms holds great promise for advanced drug delivery systems. These systems can be tailored to release therapeutic agents in response to specific biological stimuli, such as pH, temperature, or enzymes, thereby enhancing the precision and efficacy of treatments. Integrating MSNs with other nanomaterials, such as liposomes or polymers, can create hybrid systems that combine the advantages of multiple nanocarriers, potentially overcoming existing limitations in drug delivery. Functionalizing MSNs with targeting ligands, such as antibodies, peptides, or small molecules, can enhance their ability to selectively bind to specific cells or tissues, significantly reducing off-target effects and improving the therapeutic index of drugs. Additionally, MSNs can be engineered to carry imaging agents, such as fluorescent dyes or magnetic nanoparticles, enabling their use in diagnostic imaging techniques like MRI, CT, and fluorescence microscopy. These multifunctional MSNs can simultaneously serve as diagnostic and therapeutic agents, paving the way for theragnostic. The versatility of MSNs in drug delivery and diagnostics makes them suitable for personalized medicine approaches. By tailoring MSNs to carry specific drugs or diagnostic agents, treatments can be customized to individual patient needs, potentially improving outcomes and reducing side effects.

However, ensuring the biocompatibility and safety of mesoporous silica nanoparticles (MSNs) presents a significant challenge. It is critical for researchers to focus on understanding the long-term effects of MSNs in the body, including their degradation, clearance, and potential toxicity. The potential for accumulation in organs and tissues, as well as possible adverse effects from degradation products, needs to be thoroughly evaluated. Developing MSNs with coatings or surface modifications that reduce adverse immune responses and improve biocompatibility will be crucial for clinical applications.

Another major hurdle is the large-scale production of MSNs with consistent quality and reproducibility. Scaling up the production of MSNs from laboratory to industrial scale presents numerous challenges. Consistency in quality, reproducibility of synthesis methods, and cost-effectiveness are critical factors that need to be addressed. Current manufacturing processes may not yet meet the stringent requirements for large-scale production, which could impact the feasibility of MSNs for widespread clinical use. Techniques for the scalable and cost-effective synthesis of MSNs must be developed to facilitate their commercialization. Addressing issues related to batch-to-batch variability and particle size and morphology uniformity will be essential for regulatory approval and clinical use. Navigating the regulatory pathways to approve MSN-based therapies and diagnostics is complex and requires a comprehensive evaluation of their safety, efficacy, and quality.

Collaborations between researchers, industry, and regulatory agencies will be necessary to establish clear guidelines and standards for developing and approving MSN-based products.

Another challenge in using MSNs in clinical applications is that achieving stable and effective targeting of MSNs in vivo remains a challenge. The nanoparticles must navigate the complex biological environment, avoid clearance by the immune system, and reach the intended target site. The research will be critical to improving the stability of MSNs in biological fluids and enhancing their targeting efficiency through surface modifications or stealth coatings. The design and synthesis of multifunctional MSNs that combine therapeutic, diagnostic, and targeting capabilities are inherently complex. Balancing these functions while maintaining the stability and performance of the nanoparticles is a significant challenge. Future research must optimize design and fabrication processes to ensure the reliable and efficient production of multifunctional MSNs.

To address the obstacles in utilizing MSNs for biomedical purposes, future developments should concentrate on innovative synthesis techniques and novel applications. Regarding synthesis innovation, advanced functionalization methods should be explored in upcoming research. Scientists are expected to develop new functionalization approaches to boost the precision and effectiveness of MSNs. Cutting-edge techniques like site-specific functionalization and dual-functionalization strategies could allow for more accurate targeting of therapeutic agents and enhanced performance in complex biological settings. Additionally, the eco-friendly production of MSNs is becoming a crucial consideration. As environmental concerns grow, sustainable synthesis methods that minimize or eliminate harmful reagents will become more prevalent. Biologically-inspired synthesis techniques and the use of eco-friendly solvents are anticipated to become standard practices in MSN manufacturing. Progress in synthesis methods that enable scalable and cost-effective MSN production will be vital for their widespread adoption. Advancements in automated synthesis and continuous flow processes could tackle current issues related to reproducibility and manufacturing efficiency.

Given the advantages of MSNs with further modification, this nanoparticle can be primarily considered in novel biomedical applications: (1) Personalized Medicine. MSNs are poised to play a significant role in personalized medicine by enabling targeted drug delivery and diagnostics tailored to individual patient profiles. Innovations in MSNs could lead to the development of highly specific delivery systems for precision therapies, including gene editing and personalized cancer treatments; (2) Combination Therapies. The integration of MSNs with other therapeutic modalities, such as immunotherapy or photothermal therapy, could enhance treatment efficacy and reduce side effects. Future developments may focus on designing MSNs that can simultaneously deliver multiple therapeutic agents or combine therapeutic and diagnostic functions; (3) Advanced Imaging Techniques. Emerging applications in imaging, such as multi-modal imaging using MSNs, could provide more detailed and accurate diagnostic information. The development of MSNs with enhanced imaging capabilities for real-time tracking of therapeutic processes will be a key area of exploration.

6. CONCLUSIONS

In summary, mesoporous silica nanoparticles (MSNs) represent a highly versatile and promising platform for a wide range of biomedical applications, particularly in drug delivery and diagnostic imaging. Their unique structural properties, such as high surface area, tunable pore size, and functionalizable surface, allow for the precise tailoring of MSNs to meet specific therapeutic and diagnostic needs. The synthesis of MSNs allows for precise control over size, shape, and surface functionality, enabling the creation of nanoparticles tailored for specific purposes. Advanced characterization techniques, including XRD, XPS, FTIR, NMR, and fluorescence spectroscopy, provide detailed insights into the structural and chemical properties of MSNs, ensuring their suitability for various applications. In the realm of biomedicine, MSNs offer promising solutions for drug delivery and diagnostic imaging. Their high surface area, tunable pore size, and ability to be functionalized with targeting ligands facilitate efficient drug loading and targeted delivery, enhancing therapeutic outcomes while minimizing side effects. The incorporation of stimuli-responsive release mechanisms and hybrid systems further expands their utility. Moreover, MSNs' capability to carry imaging agents enables their use in diagnostic imaging, paving the way for

theranostic applications that combine therapy and diagnostics. Despite the challenges in ensuring biocompatibility, scalable production, and regulatory approval, the continued research and development of MSNs promise to revolutionize biomedical treatments and diagnostics, offering more precise and effective solutions tailored to individual patient needs.

Acknowledgement

Wahyu N Safitriono would like to acknowledge to DEXA group for providing the scholarship through DEXA Award Science Scholarship 2022.

References

[1] F. Ahmadi *et al.*, "A review on the latest developments of mesoporous silica nanoparticles as a promising platform for diagnosis and treatment of cancer," *Int J Pharm*, vol. 625, p. 122099, Sep. 2022, doi: 10.1016/J.IJPHARM.2022.122099.

[2] A. Mohan, A. Jaison, and Y. C. Lee, "Emerging trends in mesoporous silica nanoparticle-based catalysts for CO 2 utilization reactions," *Inorg Chem Front*, vol. 10, no. 11, pp. 3171–3194, May 2023, doi: 10.1039/D3QI00378G.

[3] O. A. Saputra *et al.*, "Organically surface engineered mesoporous silica nanoparticles control the release of quercetin by pH stimuli," *Scientific Reports 2022 12:1*, vol. 12, no. 1, pp. 1–15, Nov. 2022, doi: 10.1038/s41598-022-25095-4.

[4] O. A. Saputra, W. N. Safitriono, D. E. K. Maharani, A. Febiana, and F. R. Wibowo, "pH-controlled release feature of chitosan assembled silica nanoparticles containing nano-formulated curcumin over in vitro gastric and physiological condition," *Food Biosci*, vol. 53, p. 102793, Jun. 2023.

[5] F. R. Wibowo, O. A. Saputra, W. W. Lestari, M. Koketsu, R. R. Mukti, and R. Martien, "pH-Triggered Drug Release Controlled by Poly(Styrene Sulfonate) Growth Hollow Mesoporous Silica Nanoparticles," *ACS Omega*, vol. 5, no. 8, pp. 4261–4269, 2020.

[6] O. A. Saputra, W. A. Lestari, W. N. Safitriono, M. Handayani, W. W. Lestari, and F. R. Wibowo, "β-Amino alcohol-based organosilane tailored magnetite embedded mesoporous silica nanoparticles exhibit controlled-release of curcumin triggered by pH," *Mater Lett*, vol. 305, no. August, p. 130804, 2021, doi: 10.1016/j.matlet.2021.130804.

[7] S. Jafari, H. Derakhshankhah, L. Alaei, A. Fattahi, B. S. Varnamkhasti, and A. A. Saboury, "Mesoporous silica nanoparticles for therapeutic/diagnostic applications," *Biomedicine & Pharmacotherapy*, vol. 109, pp. 1100–1111, Jan. 2019, doi: 10.1016/J.BIOPHA.2018.10.167.

[8] C. T. Kresge, M. E. Leonowicz, W. J. Roth, J. C. Vartuli, and J. S. Beck, "Ordered mesoporous molecular sieves synthesized by a liquid-crystal template mechanism," *Nature*, vol. 359, no. 6397, pp. 710–712, 1992, doi: 10.1038/359710a0.

[9] P. Selvam, S. K. Bhatia, and C. G. Sonwane, "Recent Advances in Processing and Characterization of Periodic Mesoporous MCM-41 Silicate Molecular Sieves," *Ind Eng Chem Res*, vol. 40, no. 15, pp. 3237–3261, 2001, doi: 10.1021/ie0010666.

[10] J. S. Beck *et al.*, "New Family of Mesoporous Molecular Sieves Prepared with Liquid Crystal Templates," *J Am Chem Soc*, vol. 114, pp. 10834–10843, 1992.

[11] D. Zhao, Q. Huo, J. Feng, B. F. Chmelka, and G. D. Stucky, "Nonionic Triblock and Star Diblock Copolymer and Oligomeric Surfactant Syntheses of Highly Ordered , Hydrothermally Stable , Mesoporous Silica Structures," *J Am Chem Soc*, vol. 120, pp. 6024–6036, 1998.

[12] Q. Huo, R. Leon, P. M. Petroff, and G. D. Stucky, "Mesostructure Design with Gemini Surfactants: Supercage Formation in a Three-Dimensional Hexagonal Array," *Science (1979)*, vol. 268, pp. 1324–1327, 1995.

[13] D. Zhao, Q. Huo, J. Feng, J. Kim, Y. Han, and G. D. Stucky, "Novel Mesoporous Silicates with Two-Dimensional Mesostructure Direction Using Rigid Bolaform Surfactants," *Chemistry of Materials*, vol. 11, pp. 2668–2672, 1999.

[14] S. A. Bagshaw, E. Prouzet, and T. J. Pinnavaiat, "Templating of Mesoporous Molecular Sieves by Nonionic Polyethylene Oxide Surfactants," *Science (1979)*, vol. 269, pp. 1242–1244, 1995.

[15] P. T. Tanev, Y. Liang, and T. J. Pinnavaia, "Assembly of Mesoporous Lamellar Silicas with Hierarchical Particle Architectures," *J Am Chem Soc*, vol. 119, pp. 8616–8624, 1997.

[16] P. Yang, S. Gai, and J. Lin, "Functionalized mesoporous silica materials for controlled drug delivery," *Chem Soc Rev*, vol. 41, no. 9, p. 3679, 2012, doi: 10.1039/c2cs15308d.

[17] C. H. Tsai, J. L. Vivero-Escoto, I. I. Slowing, I. J. Fang, B. G. Trewyn, and V. S. Y. Lin, "Surfactant-assisted controlled release of hydrophobic drugs using anionic surfactant templated mesoporous silica nanoparticles," *Biomaterials*, vol. 32, no. 26, pp. 6234–6244, 2011, doi: 10.1016/j.biomaterials.2011.04.077.

[18] K. Suzuki, K. Ikari, and H. Imai, "Synthesis of Silica Nanoparticles Having a Well-Ordered Mesostructure Using a Double Surfactant System," *J Am Chem Soc*, vol. 126, no. 2, pp. 462–463, 2004, doi: 10.1021/ja038250d.

[19] D. Kuang, T. Brezesinski, and B. Smarsly, "Hierarchical porous silica materials with a trimodal pore system using surfactant templates," *J Am Chem Soc*, vol. 126, no. 34, pp. 10534–10535, 2004, doi: 10.1021/ja0470618.

[20] F. Gai *et al.*, "Mixed anionic surfactant-templated mesoporous silica nanoparticles for fluorescence detection of Fe^{3+}," *Dalton Trans.*, vol. 45, no. 2, pp. 508–514, 2016, doi: 10.1039/C5DT03052H.

[21] C. Gao, H. Qiu, W. Zeng, Y. Sakamoto, and O. Terasaki, "Formation Mechanism of Anionic Surfactant Templated Mesoporous Silica (AMS)," no. 5, p. 75, 2009, doi: 10.1021/cm061107+.

[22] S. K. Natarajan and S. Selvaraj, "Mesoporous silica nanoparticles: importance of surface modifications and its role in drug delivery," *RSC Adv*, vol. 4, no. 28, p. 14328, 2014, doi: 10.1039/c4ra00781f.

[23] B. G. Trewyn, I. I. Slowing, S. Giri, H.-T. Chen, and V. S.-Y. Lin, "Synthesis and functionalization of a mesoporous silica nanoparticle based on the sol-gel process and applications in controlled release.," *Acc. Chem. Res.*, vol. 40, no. 9, pp. 846–53, 2007, doi: 10.1021/ar600032u.

[24] F. R. Wibowo, O. A. Saputra, W. W. Lestari, M. Koketsu, R. R. Mukti, and R. Martien, "PH-Triggered Drug Release Controlled by Poly(Styrene Sulfonate) Growth Hollow Mesoporous Silica Nanoparticles," *ACS Omega*, vol. 5, no. 8, pp. 4261–4269, Mar. 2020, doi: 10.1021/ACSOMEGA.9B04167/ASSET/IMAGES/LARGE/AO9B04167_0008.JPEG.

[25] L. Tang and J. Cheng, "Nonporous Silica Nanoparticles for Nanomedicine Application," *Nano Today*, vol. 8, no. 3, pp. 290–312, 2013, doi: 10.1016/j.jneumeth.2010.08.011.Autogenic.

[26] W. Stöber, A. Fink, and E. Bohn, "Controlled growth of monodisperse silica spheres in the micron size range," *J Colloid Interface Sci*, vol. 26, no. 1, pp. 62–69, 1968, doi: 10.1016/0021-9797(68)90272-5.

[27] X. Lv, L. Zhang, F. Xing, and H. Lin, "Controlled synthesis of monodispersed mesoporous silica nanoparticles: Particle size tuning and formation mechanism investigation," *Microporous and Mesoporous Materials*, vol. 225, pp. 238–244, May 2016, doi: 10.1016/J.MICROMESO.2015.12.024.

[28] O. A. Saputra, F. R. Wibowo, and W. W. Lestari, "High storage capacity of curcumin loaded onto hollow mesoporous silica nanoparticles prepared via improved hard-templating method optimized by Taguchi DoE," *Engineering Science and Technology, an International Journal*, vol. 33, p. 101070, Sep. 2022, doi: 10.1016/J.JESTCH.2021.10.002.

[29] S. Rahmani *et al.*, "Synthesis of mesoporous silica nanoparticles and nanorods: Application to doxorubicin delivery," *Solid State Sci*, vol. 68, pp. 25–31, 2017, doi: 10.1016/j.solidstatesciences.2017.04.003.

[30] M. Huang *et al.*, "Dendritic Mesoporous Silica Nanospheres Synthesized by a Novel Dual-Templating Micelle System for the Preparation of Functional Nanomaterials," *Langmuir*, vol. 33, pp. 519–526, 2017, doi: 10.1021/acs.langmuir.6b03282.

[31] J. Gupta, M. Quadros, and M. Momin, "Mesoporous silica nanoparticles: Synthesis and multifaceted functionalization for controlled drug delivery," *J Drug Deliv Sci Technol*, vol. 81, p. 104305, Mar. 2023, doi: 10.1016/J.JDDST.2023.104305.

[32] M. Florensa, M. Llenas, E. Medina-Gutiérrez, S. Sandoval, and G. Tobías-Rossell, "Key Parameters for the Rational Design, Synthesis, and Functionalization of Biocompatible Mesoporous Silica Nanoparticles," *Pharmaceutics 2022, Vol. 14, Page 2703*, vol. 14, no. 12, p. 2703, Dec. 2022, doi: 10.3390/PHARMACEUTICS14122703.

[33] V. Mahalingam and M. Sivaraju, "Microwave-Assisted Sol-Gel Synthesis of Silica Nanoparticles Using Rice Husk as a Precursor for Corrosion Protection Application," *Silicon*, vol. 15, no. 4, pp. 1967–1975, Feb. 2023, doi: 10.1007/S12633-022-02153-0/METRICS.

[34] N. Thongnoppakhun, S. Amnuaypanich, J. Prakobdee, S. Rugmai, and S. Amnuaypanich, "Sonochemical synthesis of hollow mesoporous silica spheres (HMSSs) and its effective utilization for one-step synthesis of curcumin-loaded HMSSs," *Mater Chem Phys*, vol. 322, p. 129588, Aug. 2024, doi: 10.1016/J.MATCHEMPHYS.2024.129588.

[35] R. Sun, P. Qiao, Z. Wang, and W. Wang, "Monodispersed large-mesopore mesoporous silica nanoparticles enabled by sulfuric acid assisted hydrothermal process," *Microporous and Mesoporous Materials*, vol. 317, p. 111023, Apr. 2021, doi: 10.1016/J.MICROMESO.2021.111023.

[36] R. Sun, A. Zhang, H. D. Sun, J. Jiang, and W. Wang, "Facile synthesis of monodispersed mesoporous silica nanoparticles with ultra-large mesopores through a NaBH4-assisted hydrothermal process," *J Non Cryst Solids*, vol. 627, p. 122820, Mar. 2024, doi: 10.1016/J.JNONCRYSOL.2023.122820.

[37] B. D. de Greñu, R. de los Reyes, A. M. Costero, P. Amorós, and J. V. Ros-Lis, "Recent Progress of Microwave-Assisted Synthesis of Silica Materials," *Nanomaterials 2020, Vol. 10, Page 1092*, vol. 10, no. 6, p. 1092, Jun. 2020, doi: 10.3390/NANO10061092.

[38] S. R. Priyan *et al.*, "Microwave-assisted sol-gel synthesis of mesoporous NiO-decorated silica nanostructures utilizing biogenic silica source for supercapacitor applications," *J Alloys Compd*, vol. 976, p. 173206, Mar. 2024, doi: 10.1016/J.JALLCOM.2023.173206.

[39] L. Gu *et al.*, "One-pot hydrothermal synthesis of mesoporous silica nanoparticles using formaldehyde as growth suppressant," *Microporous and Mesoporous Materials*, vol. 152, pp. 9–15, Apr. 2012, doi: 10.1016/J.MICROMESO.2011.11.047.

[40] Q. Yu, J. Hui, P. Wang, B. Xu, J. Zhuang, and X. Wang, "Hydrothermal synthesis of mesoporous silica spheres: effect of the cooling process," *Nanoscale*, vol. 4, no. 22, pp. 7114–7120, Oct. 2012, doi: 10.1039/C2NR31834B.

[41] A. El-Fiqi and M. Bakry, "Facile and rapid ultrasound-mediated synthesis of spherical mesoporous silica submicron particles with high surface area and worm-like mesoporosity," *Mater Lett*, vol. 281, p. 128620, Dec. 2020, doi: 10.1016/J.MATLET.2020.128620.

[42] K. M. Alotaibi *et al.*, "Ultrasound-assisted synthesis of MSNs/PS nanocomposite membranes for effective removal of Cd2+ and Pb2+ ions from aqueous solutions," *Ultrason Sonochem*, vol. 98, p. 106497, Aug. 2023, doi: 10.1016/J.ULTSONCH.2023.106497.

[43] C. Pereira *et al.*, "Designing novel hybrid materials by one-pot co-condensation: From hydrophobic mesoporous silica nanoparticles to superamphiphobic cotton textiles," *ACS Appl Mater Interfaces*, vol. 3, no. 7, pp. 2289–2299, Jul. 2011, doi: 10.1021/AM200220X/SUPPL_FILE/AM200220X_SI_002.PDF.

[44] A. Gottuso, F. Armetta, A. Cataldo, V. M. Nardo, F. Parrino, and M. L. Saladino, "Functionalization of mesoporous silica nanoparticles through one-pot co-condensation in w/o emulsion," *Microporous and Mesoporous Materials*, vol. 335, p. 111833, Apr. 2022, doi: 10.1016/J.MICROMESO.2022.111833.

[45] G. D. Aquino, M. S. Moreno, C. M. Piqueras, G. P. Benedictto, and A. M. Pereyra, "Alternative Synthesis of MCM-41 Using Inexpensive Precursors for CO2 Capture," *Inorganics 2023, Vol. 11, Page 480*, vol. 11, no. 12, p. 480, Dec. 2023, doi: 10.3390/INORGANICS11120480.

[46] W. J. J. Stevens, K. Lebeau, M. Mertens, G. Van Tendeloo, P. Cool, and E. F. Vansant, "Investigation of the morphology of the mesoporous SBA-16 and SBA-15 materials," *Journal of Physical Chemistry B*, vol. 110, no. 18, pp. 9183–9187, May 2006, doi: 10.1021/JP0548725/ASSET/IMAGES/LARGE/JP0548725F00009.JPEG.

[47] D. Gkiliopoulos *et al.*, "SBA-15 Mesoporous Silica as Delivery Vehicle for rhBMP-2 Bone Morphogenic Protein for Dental Applications," *Nanomaterials 2022, Vol. 12, Page 822*, vol. 12, no. 5, p. 822, Feb. 2022, doi: 10.3390/NANO12050822.

[48] R. Huirache-Acuña *et al.*, "SBA-15 Mesoporous Silica as Catalytic Support for Hydrodesulfurization Catalysts—Review," *Materials 2013, Vol. 6, Pages 4139-4167*, vol. 6, no. 9, pp. 4139–4167, Sep. 2013, doi: 10.3390/MA6094139.

[49] M. M. Ayad, N. A. Salahuddin, A. A. El-Nasr, and N. L. Torad, "Amine-functionalized mesoporous silica KIT-6 as a controlled release drug delivery carrier," *Microporous and Mesoporous Materials*, vol. 229, pp. 166–177, Jul. 2016, doi: 10.1016/J.MICROMESO.2016.04.029.

[50] J. Sivaguru *et al.*, "Diamine functionalized cubic mesoporous silica for ibuprofen controlled delivery," *J Nanosci Nanotechnol*, vol. 15, no. 7, pp. 4784–4791, Jul. 2015, doi: 10.1166/JNN.2015.9811.

[51] M. Aquib *et al.*, "Targeted and stimuli–responsive mesoporous silica nanoparticles for drug delivery and theranostic use," Dec. 01, 2019, *John Wiley and Sons Inc.* doi: 10.1002/jbm.a.36770.

[52] Y. Feng *et al.*, "Mesoporous Silica Nanoparticles-Based Nanoplatforms: Basic Construction, Current State, and Emerging Applications in Anticancer Therapeutics," 2023, *John Wiley and Sons Inc*. doi: 10.1002/adhm.202201884.

[53] Y. Zhou, Q. Xu, C. Li, Y. Chen, Y. Zhang, and B. Lu, "Hollow mesoporous silica nanoparticles as nanocarriers employed in cancer therapy: A review," Dec. 01, 2020, *Higher Education Press Limited Company*. doi: 10.1007/s11706-020-0526-4.

[54] F. Farjadian, A. Roointan, S. Mohammadi-Samani, and M. Hosseini, "Mesoporous silica nanoparticles: Synthesis, pharmaceutical applications, biodistribution, and biosafety assessment," Mar. 01, 2019, *Elsevier B.V.* doi: 10.1016/j.cej.2018.11.156.

[55] M. Pérez-Garnes *et al.*, "Engineering hollow mesoporous silica nanoparticles to increase cytotoxicity," *Materials Science and Engineering C*, vol. 112, Jul. 2020, doi: 10.1016/j.msec.2020.110935.

[56] M. Ghaferi, M. Koohi Moftakhari Esfahani, A. Raza, S. Al Harthi, H. Ebrahimi Shahmabadi, and S. E. Alavi, "Mesoporous silica nanoparticles: synthesis methods and their therapeutic use-recent advances," 2021, *Taylor and Francis Ltd.* doi: 10.1080/1061186X.2020.1812614.

[57] A. Rahikkala *et al.*, "Mesoporous Silica Nanoparticles for Targeted and Stimuli-Responsive Delivery of Chemotherapeutics: A Review," Jul. 01, 2018, *Wiley-VCH Verlag*. doi: 10.1002/adbi.201800020.

[58] A. G. Shard, "A straightforward method for interpreting XPS data from core-shell nanoparticles," *Journal of Physical Chemistry C*, vol. 116, pp. 16806–16813, 2012, doi: 10.1021/jp305267d.

[59] A. J. Paul, F. Bretagnol, G. Buyle, C. Colin, O. Lefranc, and H. Rauscher, *Evaluation of Plasma-Deposited Anti-Adhesive and Anti-Bacterial Coatings on Medical Textiles*. Woodhead Publishing Limited, 2010. doi: 10.1533/9780857090348.48.

[60] M. W. Ambrogio, M. Frasconi, M. D. Yilmaz, and X. Chen, "New methods for improved characterization of silica nanoparticle-based drug delivery systems," *Langmuir*, vol. 29, pp. 15386–15393, 2013, doi: 10.1021/la402493q.

[61] S. B. Hartono *et al.*, "Functionalized large pore mesoporous silica nanoparticles for gene delivery featuring controlled release and co-delivery," *J Mater Chem B*, vol. 2, pp. 718–726, 2014, doi: 10.1039/c3tb21015d.

[62] J. Chen, M. Liu, C. Chen, H. Gong, and C. Gao, "Synthesis and characterization of silica nanoparticles with well-defined thermoresponsive PNIPAM via a combination of RAFT and click chemistry," *ACS Appl Mater Interfaces*, vol. 3, pp. 3215–3223, 2011, doi: 10.1021/am2007189.

[63] C. Bartholome, E. Beyou, E. Bourgeat-Lami, P. Chaumont, and N. Zydowicz, "Nitroxide-Mediated Polymerizations from Silica Nanoparticle Surfaces: 'Graft from' Polymerization of Styrene Using a Triethoxysilyl-Terminated Alkoxyamine Initiator," *Macromolecules*, vol. 36, pp. 7946–7952, 2003, doi: 10.1021/ma034491u.

[64] S. T. Hess, S. Huang, A. A. Heikal, and W. W. Webb, "Current Topics Biological and Chemical Applications of Fluorescence Correlation Spectroscopy: A Review," *Biochemistry*, vol. 41, no. 3, pp. 697–705, 2002.

[65] H. Ow, D. R. Larson, M. Srivastava, B. A. Baird, W. W. Webb, and U. Wiesnert, "Bright and stable core-shell fluorescent silica nanoparticles," *Nano Lett*, vol. 5, no. 1, pp. 113–117, 2005, doi: 10.1021/nl0482478.

[66] I. Roy *et al.*, "Optical tracking of organically modified silica nanoparticles as DNA carriers: A nonviral, nanomedicine approach for gene delivery," *Proceedings of the National Academy of Sciences*, vol. 102, no. 2, pp. 279–284, 2005, doi: 10.1073/pnas.0408039101.

[67] A. Burns, P. Sengupta, T. Zedayko, B. Baird, and U. Wiesner, "Core/shell fluorescent silica nanoparticles for chemical sensing: Towards single-particle laboratories," *Small*, vol. 2, no. 6, pp. 723–726, 2006, doi: 10.1002/smll.200600017.

[68] S. Kim, T. Y. Ohulchanskyy, H. E. Pudavar, R. K. Pandey, and P. N. Prasad, "Organically Modified Silica Nanoparticles Co-encapsulating Photosensitizing Drug and Aggregation-Enhanced Two-Photon Absorbing Fluorescent Dye Aggregates for Two-Photon Photodynamic Therapy," *J Am Chem Soc*, vol. 129, pp. 2669–2675, 2007.

[69] A. Master, M. Livingston, and A. Sen Gupta, "Photodynamic Nanomedicine in the Treatment of Solid Tumors : Perspective and Challenges," *Journal of Control Release*, vol. 168, no. 1, pp. 88–102, 2013, doi: 10.1016/j.jconrel.2013.02.020.Photodynamic.

[70] P. Couleaud, V. Morosini, C. Frochot, S. Richeter, L. Raehm, and J.-O. Durand, "Silica-based nanoparticles for photodynamic therapy applications," *Nanoscale*, vol. 2, pp. 1083–1095, 2010, doi: 10.1039/c005273f.

[71] R. P. Bagwe, C. Yang, L. R. Hilliard, and W. Tan, "Optimization of Dye-Doped Silica Nanoparticles Prepared Using a Reverse Microemulsion Method," *Langmuir*, vol. 20, pp. 8336–8342, 2004.

[72] S. Mohanan, X. Guan, M. Liang, A. Karakoti, and A. Vinu, "Stimuli-Responsive Silica Silanol Conjugates: Strategic Nanoarchitectonics in Targeted Drug Delivery," *Small*, p. 2301113, 2023, doi: 10.1002/SMLL.202301113.

[73] G. G. Abdo, M. M. Zagho, and A. Khalil, "Recent advances in stimuli-responsive drug release and targeting concepts using mesoporous silica nanoparticles," *Emergent Materials 2020 3:3*, vol. 3, no. 3, pp. 407–425, Jun. 2020, doi: 10.1007/S42247-020-00109-X.

[74] R. R. Castillo, D. Lozano, B. González, M. Manzano, I. Izquierdo-Barba, and M. Vallet-Regí, "Advances in mesoporous silica nanoparticles for targeted stimuli-responsive drug delivery: an update," *Expert Opin Drug Deliv*, vol. 16, no. 4, pp. 415–439, Apr. 2019, doi: 10.1080/17425247.2019.1598375.

[75] R. Salve, P. Kumar, W. Ngamcherdtrakul, V. Gajbhiye, and W. Yantasee, "Stimuli-responsive mesoporous silica nanoparticles: A custom-tailored next generation approach in cargo delivery," *Materials Science and Engineering: C*, vol. 124, p. 112084, May 2021, doi: 10.1016/J.MSEC.2021.112084.

[76] K. Wang *et al.*, "Evaluation on redox-triggered degradation of thioether-bridged hybrid mesoporous organosilica nanoparticles," *Colloids Surf A Physicochem Eng Asp*, vol. 608, p. 125566, Jan. 2021, doi: 10.1016/J.COLSURFA.2020.125566.

[77] G. Yang *et al.*, "Surface protein-retractive and redox-degradable mesoporous organosilica nanoparticles for enhanced cancer therapy," *J Colloid Interface Sci*, vol. 649, pp. 1014–1022, Nov. 2023, doi: 10.1016/J.JCIS.2023.06.173.

[78] L. Hu *et al.*, "Biodegradable polydopamine and tetrasulfide bond co-doped hollowed mesoporous silica nanospheres as GSH-triggered nanosystem for synergistic chemo-photothermal therapy of breast cancer," *Mater Des*, vol. 215, p. 110467, Mar. 2022, doi: 10.1016/J.MATDES.2022.110467.

[79] V. T. Cong, J. L. Houng, M. Kavallaris, X. Chen, R. D. Tilley, and J. J. Gooding, "How can we use the endocytosis pathways to design nanoparticle drug-delivery vehicles to target cancer cells over healthy cells?," *Chem Soc Rev*, vol. 51, no. 17, pp. 7531–7559, Aug. 2022, doi: 10.1039/D1CS00707F.

[80] X. Ma *et al.*, "Chitosan based smart polymer composites: Fabrication and pH-Responsive behavior for bio-medical applications," *Environ Res*, vol. 221, p. 115286, Mar. 2023, doi: 10.1016/J.ENVRES.2023.115286.

[81] T. Liao *et al.*, "A chitosan/mesoporous silica nanoparticle-based anticancer drug delivery system with a 'tumor-triggered targeting' property," *Int J Biol Macromol*, vol. 183, pp. 2017–2029, Jul. 2021, doi: 10.1016/J.IJBIOMAC.2021.06.004.

[82] N. A. Nasab, H. H. Kumleh, M. Beygzadeh, S. Teimourian, and M. Kazemzad, "Delivery of curcumin by a pH-responsive chitosan mesoporous silica nanoparticles for cancer treatment," *Artif Cells Nanomed Biotechnol*, vol. 46, no. 1, pp. 75–81, Feb. 2018, doi: 10.1080/21691401.2017.1290648.

[83] G. Lohiya and D. S. Katti, "Carboxylated chitosan-mediated improved efficacy of mesoporous silica nanoparticle-based targeted drug delivery system for breast cancer therapy," *Carbohydr Polym*, vol. 277, p. 118822, Feb. 2022, doi: 10.1016/J.CARBPOL.2021.118822.

[84] Y. Chen, K. Ai, J. Liu, G. Sun, Q. Yin, and L. Lu, "Multifunctional envelope-type mesoporous silica nanoparticles for pH-responsive drug delivery and magnetic resonance imaging," *Biomaterials*, vol. 60, pp. 111–120, 2015, doi: 10.1016/j.biomaterials.2015.05.003.